Reactivity of Intermediates

From synthetic applications of hydroxycarbenes towards telluryl radicals in organic chemistry

Inauguraldissertation zum Erlangen des Doktorgrades der Naturwissenschaftlichen Fachbereiche im Gebiet der Organischen Chemie an der Justus-Liebig-Universität.

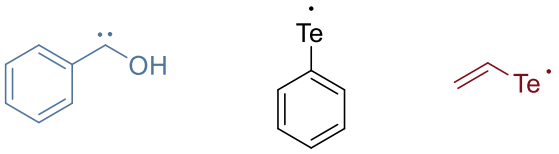

vorgelegt von

Felix Keul

angefertigt
am Institut für Organische Chemie
der Justus-Liebig-Universität
im Zeitrahmen von Dezember 2017 bis März 2022.

Betreuer: Prof. Dr. Peter R. Schreiner, PhD

Selbstständigkeitserklärung

Hiermit versichere ich, die vorgelegte Thesis selbstständig und ohne unerlaubte fremde Hilfe und nur mit den Hilfen angefertigt zu haben, die ich in der Thesis angegeben habe. Alle Textstellen, die wörtlich oder sinngemäß aus veröffentlichten Schriften entnommen sind, und alle Angaben die auf mündlichen Auskünften beruhen, sind als solche kenntlich gemacht. Bei den von mir durchgeführten und in der Thesis erwähnten Untersuchungen habe ich die Grundsätze guter wissenschaftlicher Praxis, wie sie in der ‚Satzung der Justus-Liebig-Universität zur Sicherung guter wissenschaftlicher Praxis' niedergelegt sind, eingehalten. Gemäß § 25 Abs. 6 der Allgemeinen Bestimmungen für modularisierte Studiengänge dulde ich eine Überprüfung der Thesis mittels Anti-Plagiatssoftware.

_____ _____

Datum Unterschrift

Für Hannah

Zusammenfassung

Hydroxycarbene (R–C̈–OH) waren lange Zeit nur theoretisch bekannt und als Intermediate in verschiedenen Reaktionen postuliert. Bis 2008 waren lediglich in Metallkomplexen stabilisierte Hydroxycarbene als Fischer- und Schrock-Carbene bekannt. Mit der Matrixisolationsmethode gelang es Schreiner *et al*. die freie Form des Hydroxycarbens bei Tieftemperaturen nahe dem absoluten Nullpunkt nachzuweisen. Es konnte dabei gezeigt werden, dass trotz der tiefen Temperaturen Hydroxycarbene nicht persistent sind und durch quantenmechanisches Tunneln (QMT) zu dem entsprechenden Aldehyd weiter reagieren. Ausgehend von der initialen Arbeit 2008 über das einfachste Hydroxycarben, Hydroxymethylen (H–C̈–OH), wurde in dem folgenden Jahrzehnt eine Vielzahl von Derivaten isoliert und deren Reaktivität untersucht.

In der ersten Veröffentlichung wurde erstmals ein freies Hydroxycarben in Lösung generiert und dessen Reaktionsprodukt nachgewiesen. Dazu wurde ein für die McFadyen-Stevens-Reaktion modifizierter Precursor verwendet, welcher in der Lage ist, bei 55 °C unter basischen Bedingungen unter Abspaltung einer Tosyl-Gruppe und N_2 Phenylhydroxycarben zu generieren. Dieses wurde dann in einer Carbonyl-En Reaktion mit Benzaldehyd und Aceton abgefangen, wobei das entsprechende Acetoin in NMR-Experimenten nachgewiesen wurde.

Der zweite Teil der Promotion dreht sich rund um Tellur-Radikale. Diese haben ein sehr breites Anwendungsspektrum und können sowohl in der Synthese wie Cross-Coupling-Reaktionen und Transmetallierungen, als auch industriell in der Polymerchemie verwendet werden. Die Gruppe von Yamago beschäftigt sich seit den frühen 2000ern mit Organotellurverbindungen und deren Anwendung als Radikalstarter in der Polymerchemie, jedoch wurden noch nie die entsprechenden Tellur-Radikale isoliert und untersucht.

In der zweiten und dritten Publikation geht es um diese Organotellurradikale und sowohl deren Eigenschaften als auch Reaktivitäten genau dieser Organotellur-Radikale. Aus den entsprechenden Dimeren wurde das Phenyltellurylradikal und das Vinyltellurylradikal in Matrixisolationsexperimenten dargestellt, deren Stabilität untersucht und die Reaktion mit molekularem Sauerstoff beobachtet. Während das Phenyltellurylradikal eine hohe Stabilität aufweist, zerfällt das Vinyltellurylradikal bei der Bestrahlung mit Licht zu einem Acetylen-TeH-Radikal-Komplex. In einer Reaktion mit Sauerstoff verhalten sich beide Radikale identisch. In einer barrierefreien Reaktion bilden sie zunächst ein Hyperoxid, welches anschließend zu einem Dioxid umlagert.

Abstract

Hydroxycarbenes (R–C̈–OH) were only theoretically known for a long time and postulated as intermediates in many reactions. Until 2008 only stabilized hydroxycarbenes by metal complexes as Fischer- and Schrock-carbenes are known. Schreiner *et al*. used matrix isolation methods to trap a free hydroxycarbene near absolute zero. Even at these low temperatures hydroxycarbenes turned out as not persistent and reacted by quantum mechanical tunneling (QMT) towards the corresponding aldehydes. Starting from the initial work in 2008 about the simplest hydroxycarbene, hydroxymethylene (H–C̈–OH), in the following decade a lot of derivatives were isolated and studied.

The first publication deals with the generation of free hydroxycarbenes in solution and the proof of the existence of their reaction products. A modified McFadyen-Stevens precursor was used to generate phenylhydroxycarbene under the cleavage of a tosyl-group and nitrogen extrusion. Phenylhydroxycarbene was trapped by benzaldehyde and acetone in a so-called carbonyl-ene reaction and the formation of the resulting acetoins is proven *via* NMR spectroscopy.

The second part of this thesis is about tellurium radicals. These come up with a broad spectrum of applications and are used in cross-couplings and trans-metalations as well as in industrial polymer chemistry. The group of Yamago started to study organotellurium compounds and their application in polymer chemistry in the early 2000s but the used tellurium radicals were never isolated and studied before.

In the second and third publications organotellurium radicals, namely phenyltelluryl radical and vinyltelluryl radical, are isolated and their properties and reactivities are described. We used the corresponding dimers to isolate them in an inert solid argon matrix and studied their stability and reaction with molecular oxygen. While the phenyltelluryl radical proves to be stable under matrix isolation conditions, the vinyltelluryl radical rearranges under photoirradiation towards an acetylene-TeH-radical complex. In reaction with molecular oxygen both behave identically. In a barrierless reaction, they primarily form a hyperoxide which isomerizes towards a dioxide.

Table of contents

1 Introduction

Hydroxycarbenes[1,2] with their quantum mechanical tunneling (QMT) behavior are well established since the first generation and isolation under inert/cryogenic conditions in 2008.[3] But the insight of this behavior is still lacking and their role in the origin of life is not fully understood. The aim of this thesis is to use modern methods for generating hydroxycarbenes in solution. This allows us to learn more about their stability and reactivity in general and allows us to study reactions of hydroxycarbenes in more "earth like" conditions.

The second aim of this thesis deals with tellurium-centered radicals. On the one hand, sulfur-containing radicals[4–10] have been studied in this group and appear to be relevant in atmospheric chemistry as reactants for oxygen. On the other hand, radicals that are biologically or industrially relevant, were studied as well.[11,12] Telluryl radicals are widely used in living polymerization reactions as radical starters and controlling the chain length. The isolation helps us to understand the properties and reactivities of this type of species.

1.1 Carbene chemistry

The IUPAC describes carbenes as follows:

"*The electrically neutral species H_2C: and its derivatives, in which the carbon is covalently bonded to two univalent groups of any kind or a divalent group and bears two nonbonding electrons, which may be spin-paired (singlet state) or spin-non-paired (triplet state)*."[13]

As mentioned by IUPAC, carbenes are divalent carbon atoms with six electrons. While four electrons are involved in the bonding one divalent or two univalent groups, two electrons are non-bonding and the octet rule is violated. This electron deficiency leads to their highly reactive character. In one case, these non-bonding electrons can be spin-paired, which leads to two singlet spin states ($2S + 1 = 1$; $S = 0$). The electrons are in a sp^2-orbital, while the p-orbital is unoccupied. In the other case, the free electrons are unpaired which goes hand in hand with a triplet spin state ($2S + 1 = 3$; $S = 1$). While the triplet state has only one open-shell electron configuration, there are three ($\sigma^1 p\pi^1$, p_π^2, σ^2) conceivable states for singlet carbene.

The first attempts to generate carbenes by Butlerow[14] and Nef[15–17] failed because of the lack of knowledge about their high reactivity and fast reaction times. This was demonstrated later by Curtius[18] and Staudinger[19] using diazo compounds and ketenes. The experimental evidence for the existence of methylene (H–C̈–H, **2**) was first given by Herzberg[20,21] in the middle of the 20th century.

Not only the generation of **2** was challenging but also its computations. In 1960 Foster and Boys started with their pioneering work on *ab initio* computations for **2**.[22] In the following years, many theoretical chemists[23–26] tried to compute the correct geometrical parameters but struggled with the first incorrect assumption of Herzberg of a linear triplet ground state. In 1970 two independent EPR studies from Bernheim *et al*.[27] and Wassermann *et al*.[27] proved the assumption of theoreticians correct and finally an H–C–H bond angle of 134° in an electronic triplet ground state ($^3B_1$) was confirmed, while the first excited state is singlet ($^1A_1$) with a bond angle of 102.5°. The singlet-triplet gap is approximately ΔE_{S-T} = 8.5 kcal mol^{-1}.[28,29]

Nowadays many methods for the generation of carbenes are known. A typical strategy is a usage of labile diazo compounds (**1** as the simplest example) as a precursor.[20] Thermal and/or photolytic cleavage of these compounds leads to dinitrogen extrusion and the formation of the desired carbene. Because of the high reactivity with the undesired outcome of diazo compounds, most of the time tosylhydrazones are used as a stabilized form of diazo compounds. Treating with a strong base, carbenes can be generated, which is known as the so-called Bamford-Stevens-reaction.[30]

A second procedure is the α-elimination of halogens. Dichlorocarbene (Cl–C̈–Cl, **4**) is a prominent example of a carbene, generated out of chloroform. After its first postulation in 1862,[31] dichlorocarbene was claimed as an intermediate in the hydrolysis of chloroform (**3**)[32] and finally proven by its addition to olefins.[33] Generally, 1,1-dihalocarbenes can be generated *in situ* using a base.[34,35] A rarely used, but possible way to generate carbenes is using ketenes as precursors (Scheme 1).[36]

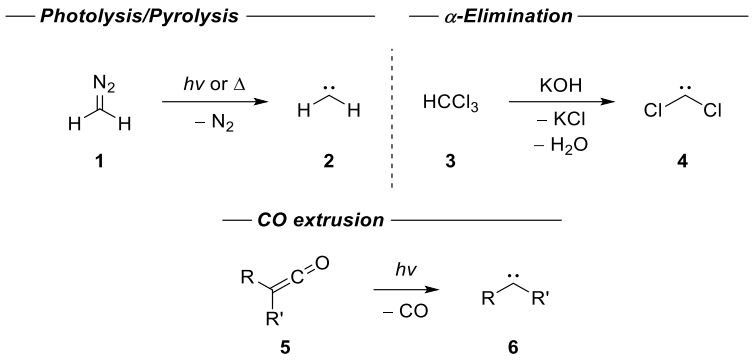

Scheme 1. Most common pathways to generate carbenes. Top left: Generation of methylene (**2**) using diazomethane (**1**) as a precursor. Top right: α-elimination of haloforms, with chloroform (**3**) as an example. Bottom: Generation of carbenes with ketenes as a precursor.

As mentioned before, carbenes have a highly reactive character and have a broad range of reactivities. In an intramolecular fashion, carbenes can rearrange in a [1,2]-shift towards alkenes.[37,38] Depending on the spin state of the carbene, they can insert into C–H and C–X bonds. While the insertion of a singlet carbene is concerted and stereospecific, the insertion of a triplet carbene is not.[39] Furthermore, carbenes are used in cycloadditions, which produce cyclopropanes and cyclopropenes using alkenes and alkynes as starting materials, respectively.[33]

Over the last decades, many carbenes were generated and spectroscopically characterized. A famous example from Giessen is cyclopropenylidene **7**,[40,41] which was prepared and trapped in an argon matrix at 10 K and was found in the interstellar medium and Saturn moon titan, as well.[42] A second example, also from Giessen, is vinylidenecarbene **8**,[43] a further molecule on the C_3H_2 hypersurface. With the isolation of propargylene **9**[41,44] the family of C_3H_2 carbene isomers is completed. The interconversion of **9** with a low-lying transition state near the vibrational ground state made the identification *via* IR spectroscopy difficult. The hetero-substituted cyclic oxiranylidene **10**,[45] which is on the same C_2H_2O hypersurface as uncharacterized formylcarbene,[46,47] was also first isolated under cryogenic conditions in Giessen. Furthermore, heteroatom-containing carbenes like oxaethenylidene **11**[48] and thiooxaethenylidene **12**[49] are found in the cold, dark molecular cloud TMC-1 (Scheme 2).

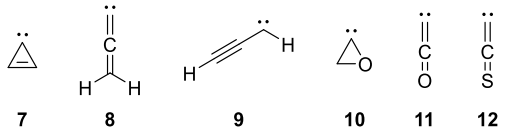

Scheme 2. Several reactive carbenes have been prepared under matrix isolation conditions.

1.2 Hydroxycarbenes

1.2.1 Hydroxycarbene chemistry

Hydroxymethylene (H–C̈–OH, **15**), the parent hydroxycarbene, was first implicated in 1921 by Barker and co-workers in the photocatalytic reaction of carbon dioxide and water.[50] Hydroxymethylene depicts a high-energy tautomer of formaldehyde[51–55] and was not isolated before 2008[3] although it should be possible.[56] Hydroxymethylene was generated through thermal CO_2 extrusion of glyoxylic acid (**13**) in an HVFP experiment at 1000 °C and trapped in a solid argon matrix at 11 K. After isolation, it was fully characterized by IR and UV/Vis spectroscopy which was supported by *ab initio* AE-CCSD(T)/cc-pCVQZ level of theory computations. The CO_2 extrusion exclusively yields the *trans* conformer of **14**, because of the five-membered cyclic transition state. An isomerization between *trans* and *cis* was not observed at 11 K due to the high barrier (26.8 kcal mol^{-1}). The rearrangement towards formaldehyde (**15**) is also not reachable in theory at these low temperatures because of the high barrier of 29.7 kcal mol^{-1}. Nevertheless, Schreiner *et al*. observed increasing bands due to **15** in the same ratio as bands of **14** decreasing. The disappearance of **14t** occurs in a measured first-order decay with a half-live of τ = 2.1 h, while deuterated **14**-*d* (H–C̈–OD) is persistent under these conditions. An explanation of this behavior is quantum mechanical tunneling (QMT) (Scheme 3).[3]

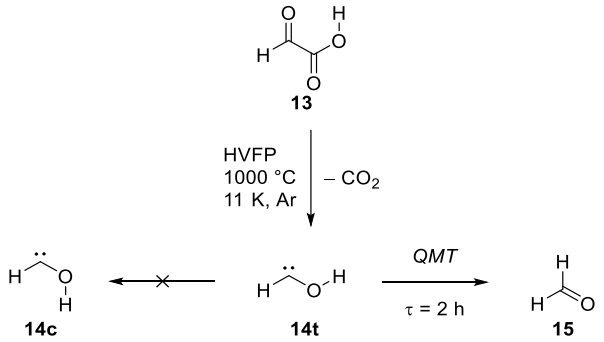

Scheme 3. Generation in HVFP at 1000 °C and subsequently trapping of hydroxymethylene **14** in a solid argon matrix at 11 K.

In the following years, the strategy of α-keto acids as precursor was used to generate and trap various substituted hydroxycarbenes and study their tunneling behavior.[1,2] Derivatives of glyoxylic acids lead to a broad range of hydroxycarbenes. The tunneling half-lives of alkyl-derivatives methylhydroxycarbene (H_3C–C̈–OH, **16**)[57] and *tert*-butyl-hydroxycarbene (($H_3C)_3C$–C̈–OH, **17**)[58] are slightly decreased with τ = 1.1 h and τ = 1.8 h, respectively, in comparison to parent **14t**, due to an inductive donating effect (+I) of alkyl groups. Contrarily, phenylhydroxycarbene (**18**) and cyclopropylhydroxycarbene (**19**) benefit from a π-donating

effect of their substituents with increased tunneling half-lives of $\tau = 2.5$ h and $\tau = 17.8$ h, respectively. Introducing electron-withdrawing substitutions like in the case of ethynylhydroxycarbene (HC≡C–C̈–OH, **20**),[59] trifluoromethylhydroxycarbene (F_3C–C̈–OH, **22**),[60] and cyanohydroxycarbene (NC–C̈–OH, **22**)[61] a push-pull system and/or captodative effect is used to slow the tunneling reaction to half-lives even further to $\tau = 3$ d, $\tau = 7$ d, and $\tau = 23.5$ d, respectively, and stabilize the labile carbene center. The hetero-substituted dihydroxycarbene (HO–C̈–OH, **23**),[62,63] methoxyhydroxycarbene (H_3CO–C̈–OH, **24**)[62], and aminohydroxycarbene (H_2N–C̈–OH, **25**)[64] only show conformational tunneling reactions between the *cis* and *trans* conformer (Scheme 4).

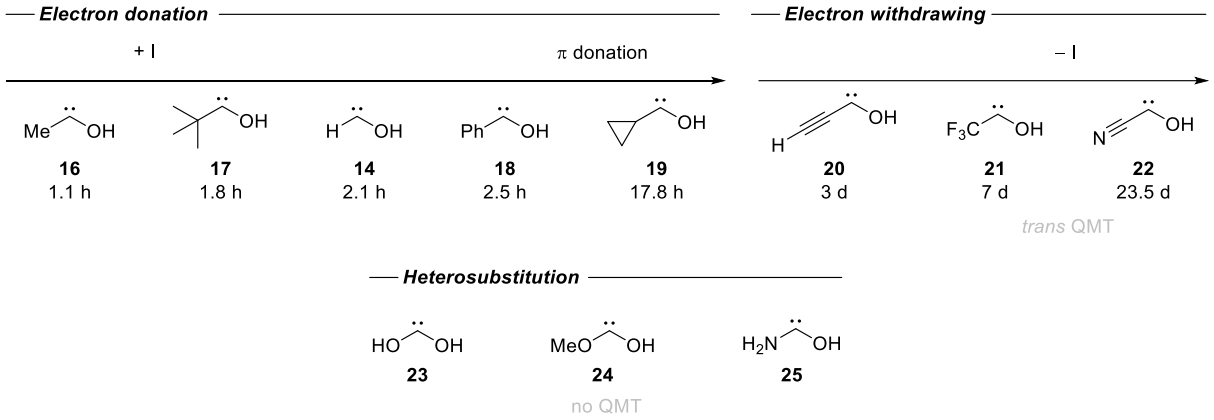

Scheme 4. Summary of matrix isolated hydroxycarbenes in the group of Schreiner with tunneling half-lives τ. Electron withdrawing groups stabilize hydroxycarbenes through push-pull effect and elongate tunneling half-lives. **20**, **21**, and **22** show conformer-specific tunneling. Heterosubstituted hydroxycarbenes **23**, **24**, and **25** show no [1,2]H-shift QMT on a laboratory timescales.

The derivative (*o*-methoxyphenyl)hydroxycarbene of **18** displays a curious case. After pyrolysis with established conditions of the corresponding α-keto acid the hydroxycarbene was not observed and the aldehyde, *o*-anisaldehyde was also not detected. Instead, the C–H insertion product 2,3-dihydrobenzofuran-3-ol was found as the major product.[65]

1.2.2 Relevance to prebiotic chemistry

Besides intramolecular reactions, hydroxycarbenes and their tautomers play a role in prebiotic chemistry. Glycolaldehyde (**26**), the first entry in the famous formose[66] (Butlerow[67]) reaction, is formally the addition product of two molecules of formaldehyde (**15**) which is chemically impossible without Umpolung. Since the formose reaction only takes place in a basic, aqueous solution in an autocatalytic[68] manner, the formation of the first molecule of **26** is a riddle until

today.[69–71] In the absence of a catalyst or Umpolung reagent a Cannizzaro reaction[72] towards methanol and formic acid is dominant. At the beginning of the 21st century, **26** was detected in space[73–76] and its formation in the absence of biological systems in a non-Earth environment was shown. Schreiner and co-workers demonstrated a possible outer-Earth mechanism for the formation of **26** with **14** involved. They showed both in matrix isolation experiments and flow pyrolysis the addition of **15** and **14** as high-energy tautomer to **26** in a nearly barrierless carbonyl-ene reaction.[77] In flow pyrolysis experiments the formation of glyceraldehyde (**28**), the next higher sugar, as the addition of **26** and **14** was observed. Furthermore, an equilibrium between 1,4-dioxolane-4-ol (**27**) and a single molecule of **15** and **26** was detected.[78] 1,4-dioxolane-4-ol (**27**) is more photostable than the dimeric counterpart and it is assumed as linking part between the aqueous formose reaction and gas-phase formaldehyde chemistry because of its capability to dimerize catalytically on surfaces (Scheme 5).[78]

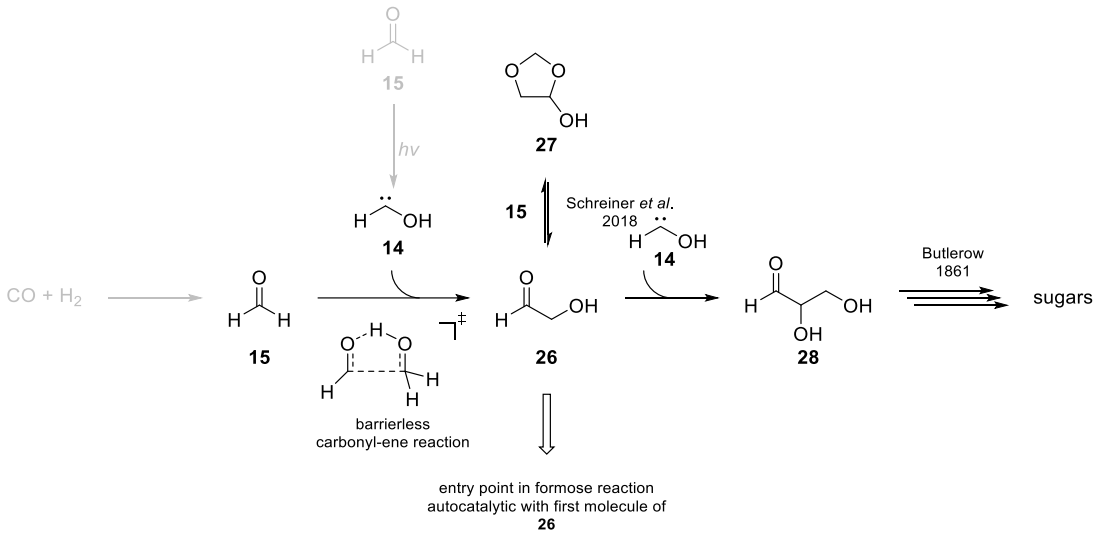

Scheme 5. Formation of glycolaldehyde (**26**) as the first entry point of the famous formose (Butlerov) reaction in a carbonyl-ene reaction between formaldehyde (**15**) and hydroxymethylene (**14**) in the gas phase. In a sugar formation iteration reaction glyceraldehyde, the C_3-sugar was also formed by the addition of **14** on **26**. An equilibrium between 1,4-dioxolane-4-ol (**27**) as storage form and **15** and **26** was observed.

Glyoxylic acid (**13**) and derivatives are not only precursors for hydroxycarbenes in matrix isolation experiments for gas-phase chemistry. Kaiser and co-worker confirmed the formation from acyl radicals in interstellar ices.[79,80] The kinetic products, enols and hydroxycarbenes, as well play a key role in prebiotic chemistry.[80] Ethenol, the corresponding enol of **16** was first detected in Sagittarius B2.[81] The higher substituted enols ethene-1,1-diol,[82,83] ethene-1,1,2-

triol,[84] and 1-aminoethenol[85] were generated and studied by the groups of Schreiner and Kaiser. It is suggested that those enols are involved in sugar-forming reactions (Scheme 6).[86]

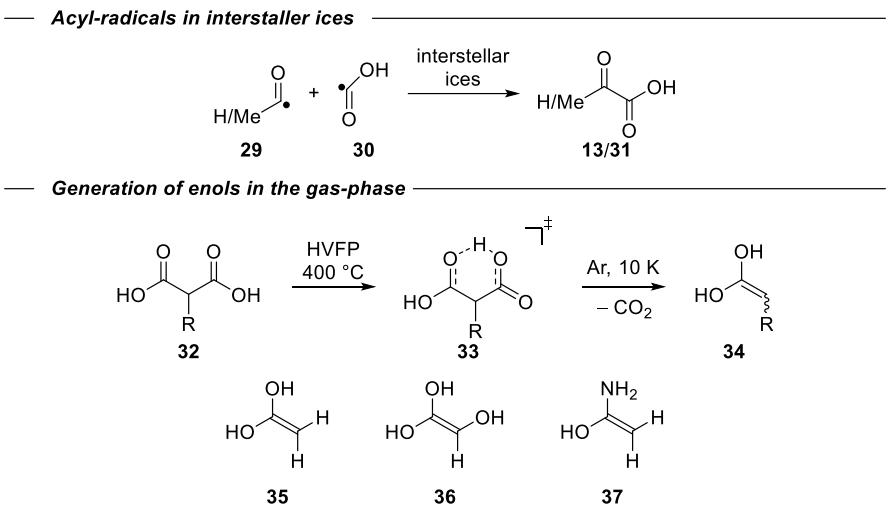

Scheme 6. Top. Formation of **13** and **31** in interstellar ices starting from acyl-radicals. Bottom: Generation of enols by HVFP at 400 °C and trapping at 10 K in inert argon matrices. **35** was also synthesized in interstellar ices.

1.3 Reactive carbenes in solution

1.3.1 Stable carbenes

Carbenes are highly reactive molecules and are usually only observable in inert conditions at low temperatures. Attempts to synthesize a stable carbene under ambient conditions were reported in 1962 by Wanzlick on *N*-heterocyclic carbenes (NHCs). He reported an equilibrium between monomeric carbene and the dimeric form of 1,3-diphenylimidazolidinylidene (**38**).[87] In 1988 Bertrand and co-worker published the generation of [bis(diisopropylamino)-phosphino]trimethylsilylcarbene (**39**), the first carbene, which is stable for several weeks under ambient conditions.[88] The double π donating interactions of the two nitrogen atoms and the carbene center by lone pair electron donation stabilize the carbene.[88] Three years later, based on the work of Wanzlick, Arduengo reported the 1,3-di-1-adamantylimidazol-2-ylidine (**40**), the first 'bottleable' NHC, which was later called Arduengo-carbene.[89] This carbene is stabilized by the π-donating effect of both nitrogen atoms next to the carbene center and aromaticity by introducing a double bond in comparison to **38**. The bulky adamantyl-groups, located on both nitrogen atoms suppress the Wanzlick-dimerization. This type of chemistry is further accomplished by Enders and co-worker with the first commercially available NHC 1,3,4-triphenyl-4,5-dihydro-1H-1,2,4-triazol-5-ylidene (**41**).[90] The latest milestone was

achieved by Bertrand *et al.* with the preparation of the first monosubstituted stabilized aminocarbene **42** (Scheme 7) in 2018.[91]

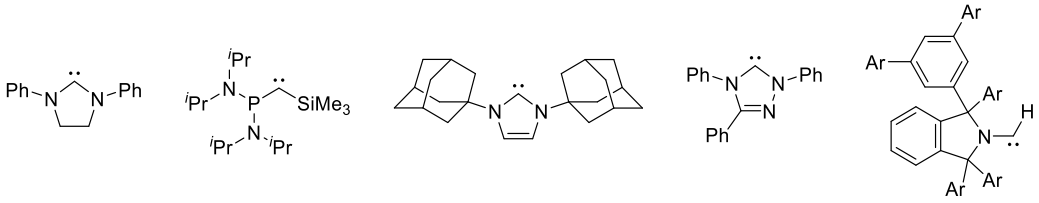

38 Wanzlick 1962 **39** Bertrand 1988 **40** Arduengo 1991 **41** Enders 1995 **42** Bertrand 2018

Scheme 7. Stabilized carbenes under ambient conditions.

1.3.2 Synthetic applications of carbenes

Next to their key role as stabilized carbenes, NHCs are also important in a broad range of reactions, *e. g.,* Umpolung reactions, oxidative acylations, and annulations.[92–94] Besides this, NHCs also play a role in biological systems in form of the coenzyme thiamine (vitamin B1). Thiamine is converted by the enzyme thiamine diphosphokinase into thiamine pyrophosphate (TPP) which is involved in glycolysis and transketolase reactions.[95] Furthermore, thiamin (**43**) is also usable in Umpolung reactions due to treating it with the base to generate the free carbene.[96] following a nucleophilic attack NHCs form the so-called Breslow intermediate by attacking a carbonyl center with a successive H-shift. It is named after Ronald Breslow after his pioneering work on these types of molecules.[97–99] After the first postulation, several attempts to isolate and/or characterize the Breslow intermediate were made, but only recently in 2018 Berkessel *et al*. were successful to generate and characterize a Breslow intermediate (**44**) by introducing the electron-withdrawing group $-CF_3$ (Scheme 8: Top).[100,101]

Stabilized carbenes within metal complexes are widely used in metathesis.[102,103] Fischer-carbenes (**45**),[104–107] named after Ernst Otto Fischer who developed these types of metal complexes for the first time, are carbene ligands with σ donor and π acceptor ligands. Because of the weak π back donation of the metal, they are slightly electrophilic. This leads to a wide application in organic reactions like Michael addition,[108] Diels-Alder reaction,[109] and Wulff-Dötz reaction.[110] In general, Fischer-carbenes are organometal complexes of hydroxycarbenes. Fischer-carbenes are not the only metal-bound carbenes. Schrock-carbenes (**46**), which are stabilized by electron donation from a metal atom into the carbene center, are the counterpart of Fischer-carbenes causing their nucleophilicity.[111] The difference between these two types of carbenes is the absence of heteroatoms. Next to their usage in metathesis,[112–114] a well-known Schrock-carbene is the Tebbe-reagent (**47**),[115] an important synthetic tool to introduce

a methylene group on ketones or esters in a Wittig[116]-type reaction. A further milestone was the development of Grubbs I and Grubbs II (**48**) as the first enantioselective catalysts.[117–119] Both catalysts tolerate many functional groups, do not need inert conditions, and are usable in a wide range of solvents.[102] The Hoveyda-Grubbs catalysts, which are based on a chelating isopropoxy group attached to the phenyl group, are also commonly used, because of their increased stability in comparison to Grubbs catalysts (Scheme 8: Bottom).[114,120,121]

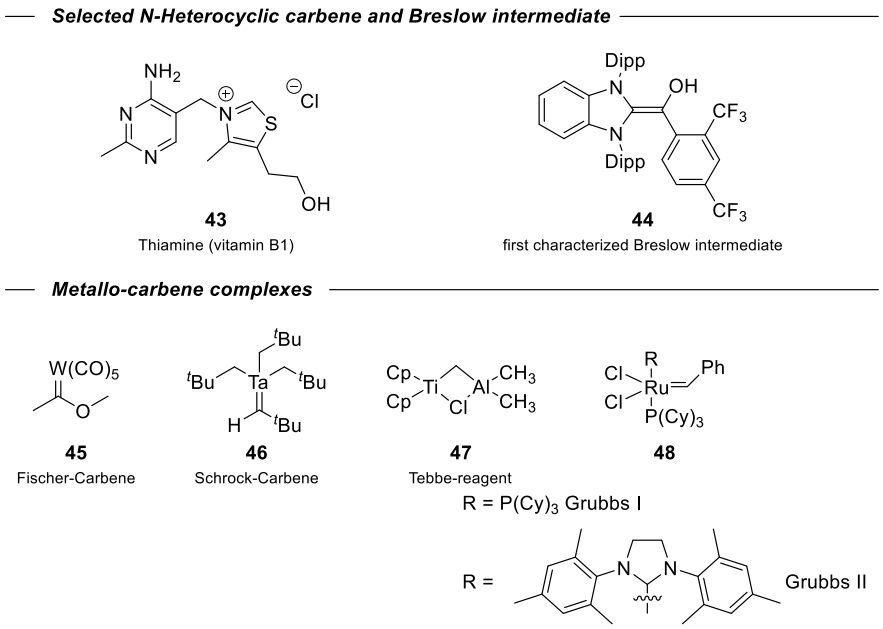

Scheme 8. Top: Thiamine (vitamin B1) and the first generated and characterized Breslow intermediate. Bottom: Metallo-carbene complexes. From left to right: The first Fischer-carbene, the first Schrock-carbene, commercially available Tebbe-reagent, and Grubbs I and Grubbs II catalysts for metathesis.

1.3.3 Generation of hydroxycarbenes in solution

In previous studies the reactivity of hydroxycarbenes and their role in prebiotic chemistry are only investigated under matrix isolation conditions at low temperatures (3-10 K). These conditions are not applicable to terrestrial environment and the reactivity under these conditions cannot be directly compared. The key question whether hydroxycarbenes may play a role in terrestrial environment for building biologically relevant molecules. As part of this thesis, we showed a proof-of-concept for the reactivity of hydroxycarbenes in a solution. The established precursor for hydroxycarbenes (*vide supra*) is not suitable for two reasons. First, free hydroxycarbenes are easily protonated by the α-keto acid starting material. Second, the activation barrier for CO_2 extrusion is $E_A \approx 40$ kcal mol^{-1} and is performed at temperatures between 600 °C - 1000 °C, which are not reachable in solution. In 2013 Fukuyama and co-

worker reported a modified precursor for the McFadyen-Stevens reaction[122,123] which operates at slightly elevated temperatures (55 °C) under weakly basic conditions.[124] Furthermore, mechanistic studies on this reaction imply the involvement of hydroxycarbenes in this reaction.[124–126] We used this type of precursor to generate **18** and derivative **52b** in solution. In the first reaction step, precursor **50** is deprotonated by imidazole and in a follow-up reaction, the tosyl group is eliminated. The formed intermediate **51** reacts similarly to α-keto acids. In a five-membered-cyclic transition state with a barrier of 30.9 kcal mol^{-1} at DLPNO-CCSD(T)/cc-PVQZ//B3LYP/def2-TZVP including SMD solvent model (toluene) nitrogen is released and the corresponding hydroxycarbenes are generated. The computed tunneling half-lives for the [1,2]H-shift of **18** and **52b** are very short with 84 s and 41 ns, at the B3LYP/def2-TZVP[127] level of theory using canonical variational theory (CVT) in conjunction with small curvature tunneling (SCT).[128] Nevertheless, we were able to prove the existence of **18** and **52b** in solution by trapping them with benzaldehyde and acetone in a carbonyl-ene reaction (Scheme 9).[129]

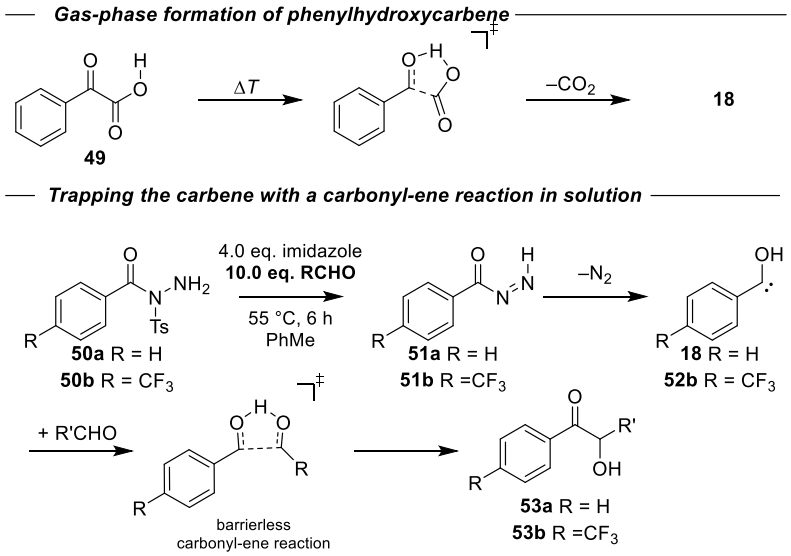

Scheme 9. Top: Phenylglyoxylic acid (**49**) as the precursor for **18** in the gas phase. Bottom: New precursors (**50**) for the generation of **18** and **52b** in solution and following trapping with an aldehyde in a carbonyl-ene reaction.

1.4 Tellurium in organic chemistry

Tellurium is a rare heavy metal element and therefore widely uncommon in organic chemistry. Like hydroxycarbenes, *vide supra*, these electron deficient radicals can also be generated and characterized by matrix isolation techniques and are also referred to as reactive intermediates. While hydroxycarbenes represent the origin of life, organotellurium compounds are crucial for higher evolved organism (*vide infra*).[130,131] Moreover, organotellurium compounds are relevant as bioactive compounds carried out in stereoselective cross-coupling reactions and are used as radicals in living polymerization reactions.[132,133,134]

1.4.1 Biological activities

Tellurium-containing compounds were postulated as highly toxic but were proposed to play a role in biological systems[130] and a typical human body possesses >0.5 g of tellurium.[131] The biological activity upon the inhibition of the growth of *B. coli communis* of tellurium compounds was already studied in the early 20th of the last century by Gilbert T. Morgan focusing on tellurium derivatives of aliphatic β-diketones (**54**, **55**).[132,135] In 1932 Fleming *et al.* showed a comparable sensitivity of bacteria between penicillin and tellurite.[136,137] The excessive usage of antimicrobial agents leads to an increased number of drug-resistant pathogens with the limiting effect of treatments. The antibacterial and antimicrobial effect of tellurium-containing compounds is a potential solution and is focused by scientists. Tellurium nanoparticles show an antibacterial effect and biofilm eradication against *E. coli*, *Pseudomonas aeruginosa*, and *S. aureus*[138] and AS101 (ammonium trichloro(dioxoethylene-O,O′-)tellurate, **56**) shows inhibition of the growth of antibiotic-resistant *Klebsiella pneumoniae*.[139] Furthermore, antibacterial activity towards gram-negative *E. coli* cells of tellurium-containing fiber meshes was reported[140] and tellurium compounds based on pyrazole derivatives show in some cases a higher antibacterial activity even than amoxicillin.[141]

Besides antibacterial activity, small organic tellurium compounds show the same trend as selenium compounds in antioxidant and anticancer activity. The pharmaceutically active compound AS101 is widely used in medicine. It is usable as an immunomodulator as a potential therapeutic drug against cancer,[142,143] autoimmune,[144] and kidney disease,[145] and at least AS101 inhibits IL-10 resulting in increased survival of tumor-bearing mice.[146] Also, arylated tellurium compounds show antioxidant activity. A broad range of tellurium-containing compounds like steroids, amino acids, nucleic bases, and polyamines are reported by Engman and co-worker and show inhibition of thioredoxin reductase and cancer cell growth.[147] Diethyl-2-phenyl-2-tellurophenyl vinylphosphate (**57**) is also a potential antioxidant against

quinolinic acid and sodium nitroprusside in the glutamatergic system, a target system in neurodegenerative diseases.[148] Laden and Porter reported the inhibition of human squalene monooxygenase by small tellurium-containing compounds, e. g., dimethyl telluride, dimethyl tellurium dichloride and tellurite (TeO_3^-).[149]

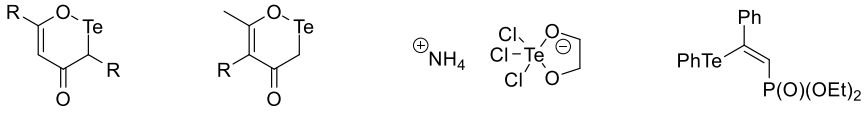

Scheme 10. Selected bioactive tellurium compounds.

1.4.2 Organotellurium compounds

Besides bioactivity, the potential of organotellurium compounds was recognized in organic chemistry. The preparation of those compounds typically started with nucleophilic tellurium reagents like Na_2Te,[150] or using elemental tellurium in a one-pot procedure with diethyl phosphite and NaH in EtOH,[151] both leading to diaryl tellurides and diaryl ditellurides. Grignard-reagents react with elemental tellurium and subsequent oxidation with air towards the corresponding ditellurides.[133] Aryl tellurides can be further used in carbotelluration and aryltelluro group transfer on alkynes using a radical starter like AIBN.[152,153] Alkyl tellurols are accessible by the reaction of elemental tellurium with alkyl lithium compounds in the presence of a proton source.[154] Finally, a reduction of organyl tellurium halides is possible to achieve diorganyl tellurides.[155,156]

Inorganic tellurium compounds like Na_2Te and NaHTe are also usable in reductions of aromatic aldehydes, double bonds, and nitriles, while aziridine sulfonates rearranges towards allylic amines.[157–159] Furthermore, Na_2TeO_2 is a mild and sensitive oxidant of thiols.[160] Next to inorganic tellurium compounds, tellurium organyls have a broad range of synthetic applications. Dibutyl tellurium methylids can be used in a Wittig reaction with aldehydes or ketones towards the corresponding olefin. Huang *et al.* described this Wittig reaction with good yields and a dominant *E* selectivity of the olefins.[161] In a similar manner dibutyl telluronium salts are used as catalysts because the generated telluroxide is reducible by triphenyl phosphite.[162] Furthermore, diphenyltelluronium methylide generates epoxides *via* reaction with the corresponding aldehydes and ketones, but needs to be prepared *in situ*.[163] A common synthetic application of tellurium compounds is the Te/Li exchange. The one-pot generation of allyl- and benzyllithium compounds with following trapping with electrophiles is well known.[164,165] Furthermore, aryltellurium compounds play a role in cross-coupling reactions.

Kang and co-workers reported cross-coupling between diaryl- and divinyl tellurium dichlorides with organostannanes in the presence of palladium or copper,[166] while Zeni and co-workers described a copper-catalyzed cross-coupling towards alkynyl tellurides, a novel class of antidepressant-like compounds.[167] Organotellurium compounds are also used in Sonogashira[168] and Suzuki-Miyaura cross-coupling reactions.[169]

1.4.3 Radical chemistry of tellurium compounds

The most common application of organotellurium compounds is in radical chemistry. Alkyl anisyl telluride (**60**) acts as a radical exchanger. In the presence of *N*-hydroxy-2-thiopyridone (**58**), a typical precursor of methyl-radical, irradiation generates methyl anisyl telluride (**61**) and an alkyl radical.[134] This strategy is used in the addition of carbohydrates to olefins,[134] synthesis of cyclic nucleosides,[170] and in intramolecular cyclization reactions (Scheme 11).[171] Next to radical exchange, acyl tellurides generate acyl radicals *via* irradiation and are highly efficient in radical cyclizations.[172]

Around 2000 a hot topic was radical-mediated group transfer with tellurium-containing compounds. Yamago and co-workers described a series of radical-mediated imidoylations. The insertion of isonitriles into a glycosidic C-Te bond is possible by using only light and heat in moderate yields around 65%. The reaction proceeds over a homolytic C-Te bond cleavage, consecutive recombination with isonitriles, and a chain termination reaction with telluryl radical.[173] The same method is applied in a more general imidoylation of acyl tellurides towards α-acyl imines with a broad scope of aliphatic, olefinic, and aromatic acyl compounds.[174,175]

In a closely related way, carbonyl compounds are activatable by silyltellurides in a three-component coupling. Heating up $Me_3SiTePh$ (**62**) leads to a silyl-radical (**64**) and forms a siloxy-radical with a carbonyl compound (**65**) in the first step (**66**). In the second step, the resulting radical yields alkynes an allylic-radical which performs a group-transfer reaction with **63** to form tellurium compound **68**.[176] This concept is extended by a change from alkynes to isocyanides yielding silylated imidoyl derivatives (**69**) (Scheme 11).[177]

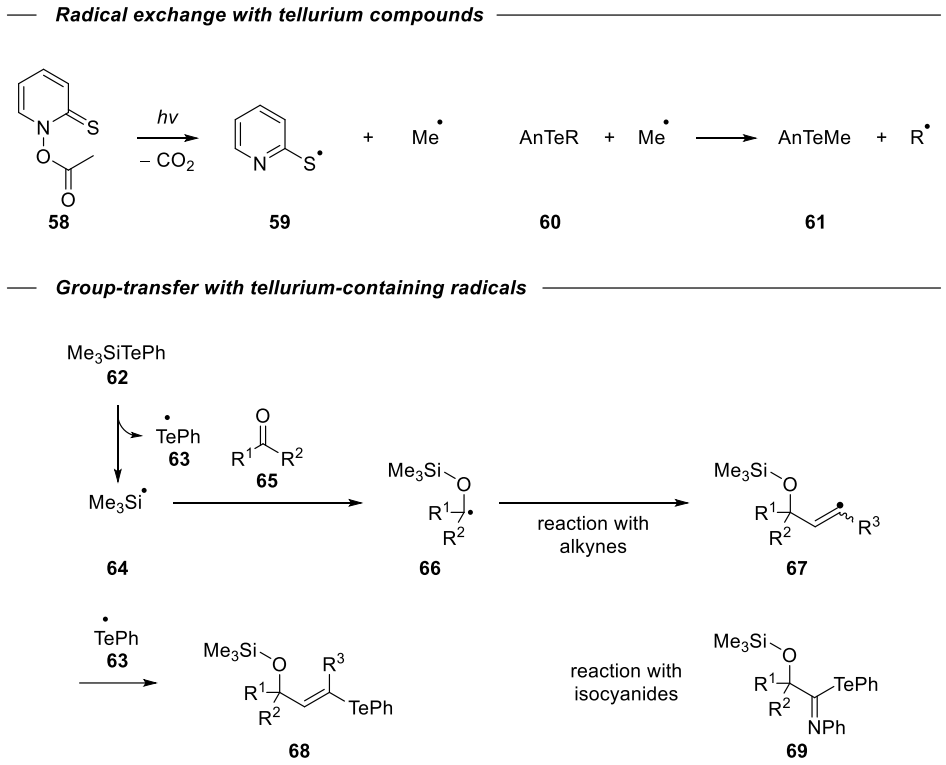

Scheme 11. Generation of methyl-radical and alkyl anisyl telluride as radical exchanger and group-transfer with tellurium-containing radicals.

As part of this thesis, we generated phenyltelluryl-radical **63** by using high vacuum flash pyrolysis of the corresponding dimer diphenyl ditelluride (**70**) and trapped it in an inert solid argon matrix at 10 K. This allowed the spectroscopic characterization by IR and UV/Vis spectroscopy for the first time.[178] The isolation of **63** also opens the possibility to study its reaction with oxygen. It is an important reaction, because it is described as an inhibitor in living polymerization reactions. In a primary reaction, the telluryl-radical forms with oxygen hyperoxy-compound **71** and after following irradiation it rearranges towards phenyltelluroyl-radical **72** (Scheme 12, Figure 1). Computations of the spin density of **71** and **72** show, in contrast to **63**, that the free electron is mostly located at oxygen atoms and, therefore, reactions involving telluryl-radicals as radical starter are inhibiting.

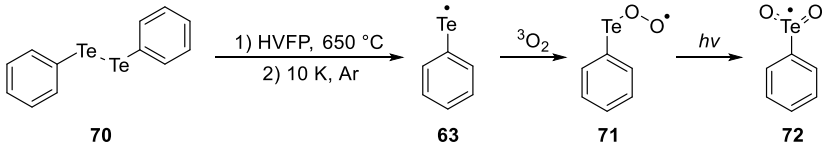

Scheme 12. Overview of the generation of **63** and its subsequent reaction with molecular oxygen.

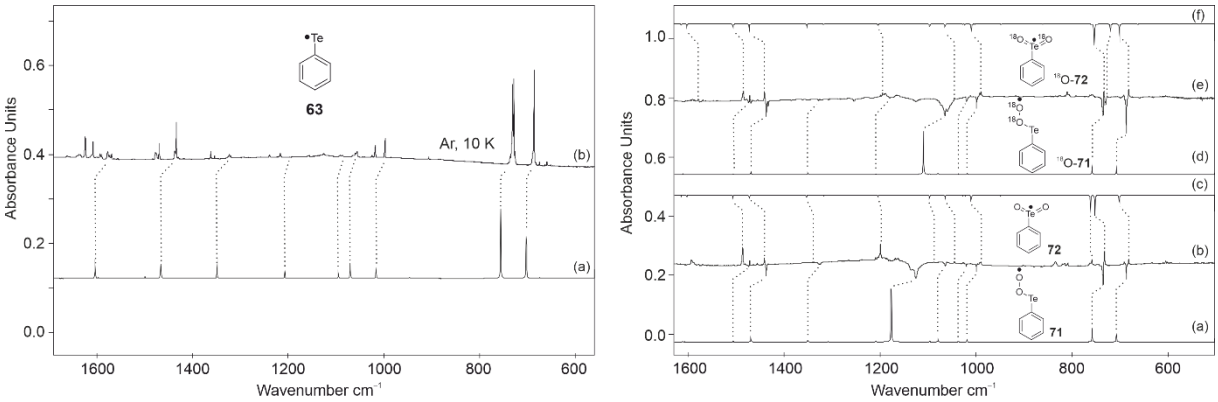

Figure 1. Left: (a) Harmonic IR spectrum of **63** computed at UB3LYP/def2-QZVPP (unscaled); (b) IR spectrum of matrix isolated compounds after pyrolysis of **70** in Ar at 10 K; the pyrolysis temperature was 650 °C; right: (a) Computed harmonic IR spectrum of **71**; (b) IR difference spectrum after photoirradiation with a wavelength of λ = 436 nm in Ar at 10 K. Downward assigned bands of **71** disappear, upward appearing bands are assigned to **72**; (c) computed IR spectrum of **72**; (d) computed IR spectrum of ^{18}O-**71**; (e) IR difference spectrum after photoirradiation with a wavelength of λ = 436 nm in Ar at 10 K. Downward bands assigned to ^{18}O-**71** disappear, upward bands are assigned to ^{18}O-**72**; (f) computed IR spectrum of ^{18}O-**72**. All computations were done at the UB3LYP/def2-QZVPP level of theory and the spectra are unscaled.

Furthermore, organotellurium radicals are a versatile tool in living radical polymerizations. The so-called organotellurium-mediated radical polymerization (TERP) is used in industry. This motif was introduced by Yamago and a co-worker for the first time in 2002.[179] Methyl tellurides and phenyl tellurides (**73**) with BDEs in the range of 27 – 29 kJ mol^{-1} are used in bulk polymerization of styrene and leading to molecular weights (M_n) above 10,000 and polydispersity (PD) between 1.17 and 1.80 with high conversions.[179] The generality of TERP was further studied by using methyl tellurides as an initiator in polymerization reactions with methyl acrylate and derivatives. With these initiators in hand, it is even possible to prepare the AB diblock copolymer of styrene (**76**) and methyl acrylate in an efficient manner with M_n over 20,000.[180] In general, the carbon – tellurium bond of initiators **81** – **85** is homolytically cleaved by pyrolysis or with radical starters. Carbon radical **75** initiates the radical chain, while the generated methyltelluryl- or phenyltelluryl-radicals possesses two roles. These radicals behave, on the one hand, as capping reagents of the polymer end radicals and, on the second hand, the equilibrium between **77** and **79** is responsible for the chain reaction.[180] Initiator **85** can be also generated *in situ* by using the corresponding dialkyl ditelluride and an equimolar amount of AIBN (Scheme 13).[181]

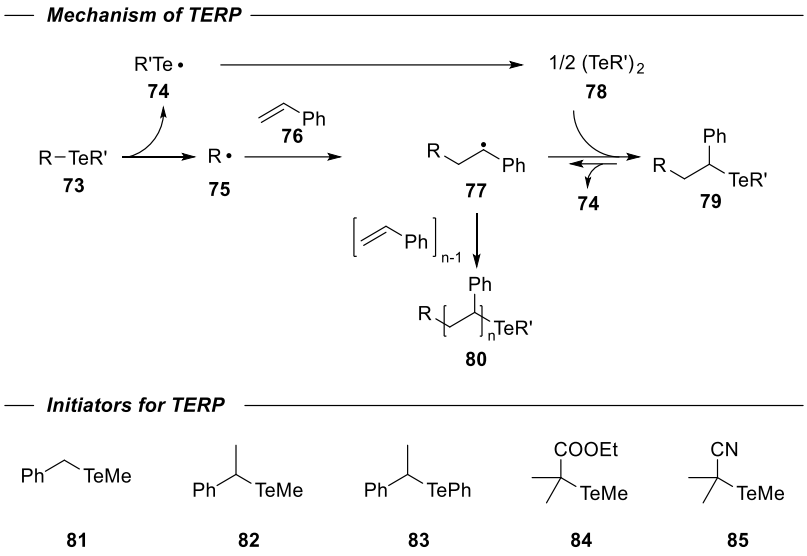

Scheme 13. Proposed mechanism of TERP and the first developed organotellurium initiators for living radical polymerization.

In the following years, the variety of monomers with different reactivities was expanded. Next to **76** and methyl acrylates, vinyl ethers,[182] fluorinated acrylates and 6-methyleneundecane,[183] 1-octene,[184] acrylonitrile and acrylamides,[185] vinylamines and vinylamides,[186] and branched polystyrenes are using dienyl telluride monomers.[187] Vinyl ethers, alkenes, and also acrylonitriles, and acrylamides can be copolymerized with methyl acrylates.[182–185] Besides copolymerization, TERP allows the one-pot synthesis of thermoresponsive diblock copolymers with *N*-vinyl-2-pyrrolidone and *N*-isopropylacrylamide as monomers. Dependent on the composition of diblock copolymers, they dissolve in water below a defined temperature and form micelles above this temperature.[188] Organotellurium-mediated radical polymerizations additionally allow the production of rigid, highly crosslinked polymer monoliths. *N,N*-methylenebis(acrylamide) forms polymeric monoliths with a controllable pore size by TERP and are usable in aqueous systems.[189] The fabrication of 3D-polymer structures with controllable pore size is also possible by using divinylbenzene and methacrylate-based monomers.[190,191] Next to monoliths, immobilized organotellurium chain transfer agents allow the formation of brushes on silicon wafer and SiPs using monomers like styrene, methyl methacrylate, and *N*-vinylpyrrolidine.[192] Monomers with a hierarchical reactivity lead to hyperbranched polymers with defined 3D-structure. These monomers are formed in copolymerization of vinyltelluride and methacrylate derivatives.[193]

As already mentioned, vinylic organotellurium compounds are involved in synthetic reactions and polymerization reactions. As part of this PhD thesis, we generated vinyltelluryl-radical **86**

by pyrolysis of the corresponding dimer divinylditelluride and trapped it in a solid argon matrix at 10 K. After irradiation with light with a wavelength of λ = 365 nm, we observed dissociation towards acetylene…TeH-radical complex **87**, which was also generated by direct photolysis of deposited divinyl ditelluride (Figure 2). The C-Te bond fission takes place in a [1,3]H-shift with a barrier of 55.5 kcal mol^{-1}. The formed vinylic TeH-radicals are not observed in matrix isolation experiments and over a low-lying saddle point **87** formed. According to computations at the UB3LYP/def2-QZVPP level of theory, the spin density is mostly localized at the tellurium-atom and NRT analysis supports this assumption. In a consecutive reaction of **86** with molecular oxygen in an initial step, the hitherto unknown vinyltelluryl hyperoxy radical was formed. Upon photoisomerization with light with a wavelength of λ = 523 nm the hyperoxy radical rearrange towards the more stable novel vinyltelluroyl radical with a barrier of 15.3 kcal mol^{-1}.[194]

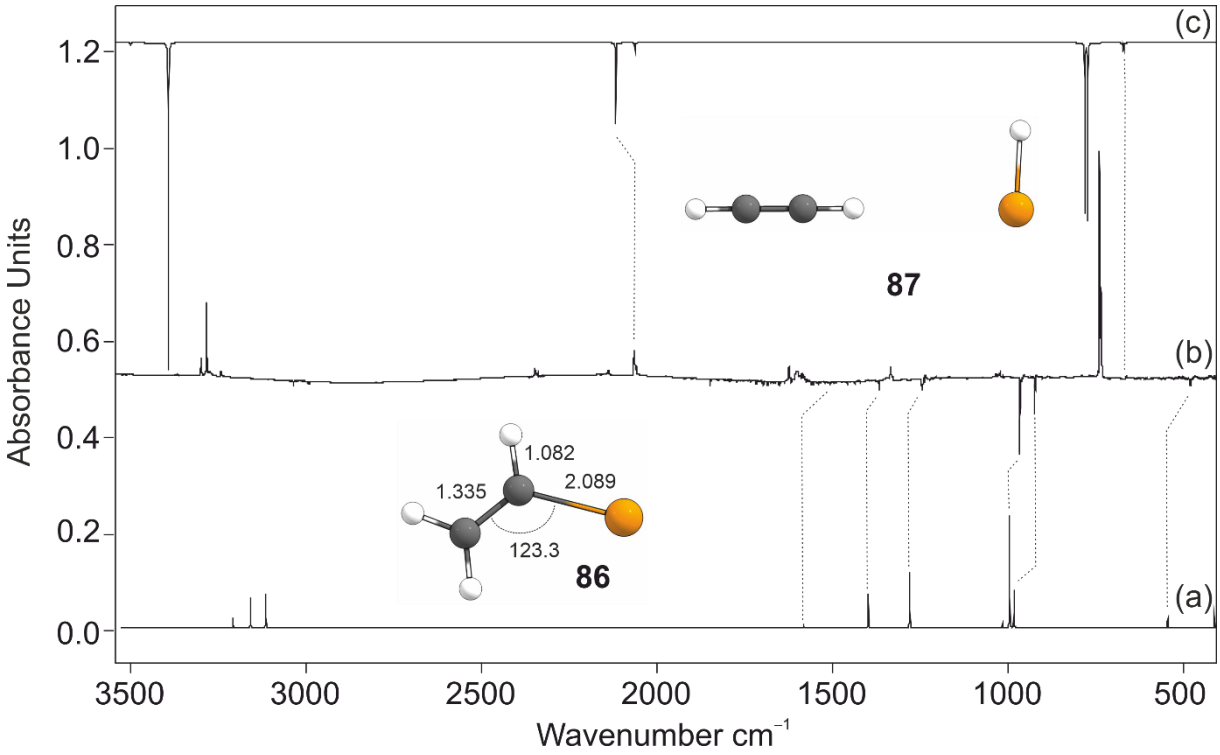

Figure 2. IR spectra showing the pyrolysis products of **86** upon subsequent trapping in an argon matrix at 10 K. (a) IR spectrum of **86** computed at UB3LYP/def2-QZVPP (unscaled). (b) IR difference spectrum showing the photochemistry of **86** after irradiation with λ = 365 nm in argon at 10 K. Downward bands assigned to **86** disappear while upward bands assigned to **87** appear after 15 min irradiation time. (c) IR spectrum of **87** computed at UB3LYP/def2-QZVPP (unscaled).

1.5 Concluding remarks and outlook

1.5.1 Hydroxycarbenes in solution

During this thesis phenylhydroxycarbene **18** and its *p*-trifluoromethyl derivative were generated by using different McFadyen-Stevens precursors in solution. A direct characterization *via* typical analytical methods is not possible because of low tunneling half-lives $\tau \approx 2$ h at 10 K[195] and even lower tunneling half-lives of $\tau = 84$ s and $\tau = 41$ ns, respectively at temperatures of 55 °C.[129] Therefore, the generated hydroxycarbenes must be trapped in solution. Benzaldehyde and acetone react as useful trapping agents. The hydroxycarbenes are trapped in a nearly barrierless carbonyl-ene reaction to the corresponding acetoin derivatives with yields between 6 and 15%. The findings are well supported by computations at DLPNO-CCSD(T)/cc-pVQZ//B3LYP/def2-TZVP level of theory.[129]

This proof-of-concept can be extended by introducing more precursors. Precursors are easily available by classical coupling reaction and following Boc-deprotection (Scheme 14). Precursors **91** and **92** extend the scope of this type of reaction and already are also used in gas-phase chemistry,[77] while the negative inducing (–I) effect of precursors **93** and **94** stabilizes the carbene center. The nitrile group of **94** also stabilizes the carbene center *via* the push-pull effect.[61] The *o*-methoxy derivative (**95**) of **49** can undergo an intramolecular C-H-insertion towards the corresponding 2,3-dihydrobenzofuran-3-ol which was already observed in the gas-phase.[65] Introducing these hydroxycarbenes helps to understand the reactivity and tunneling behavior of this type of carbenes even more. Beyond that, the presence of hydroxycarbenes, especially **14** and **16**, in solution supports the suggestion of a sugar-forming iteration reaction of hydroxycarbenes and formaldehyde and might be helping to confirm 1,3-dioxolan-4-ol (**27**) as a storage compound and entry point of formose reaction between gas- and aqueous phase.

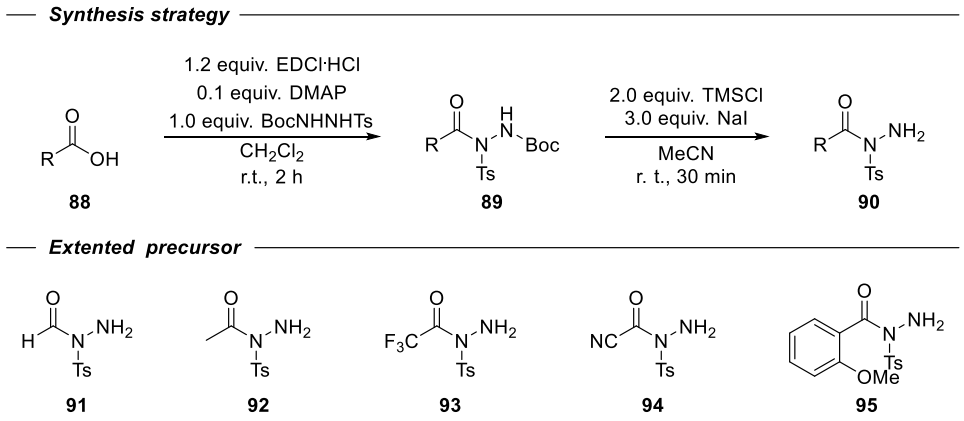

Scheme 14. Synthesis of McFadyen-Stevens precursors and new different precursor to extend the scope of the application of hydroxycarbenes in solution.

In addition to different hydroxycarbene precursors in solution, trapping agents can also be exchanged by smaller molecules like formaldehyde (**15**) or acetaldehyde (**96**). In combination with **91** as precursor trapping with **15** leads to formation of glycolaldehyde (**26**) in solution as starting point for a sugar forming iteration reaction. Also, the generation of methylhydroxycarbene (**16**) in solution by using **92** and trapping with **15** and **96** leads to hydroxyacetone (**97**) and acetoine (**98**), respectively (Scheme 15). The formation of both molecules is already proven in gas-phase chemistry.[77]

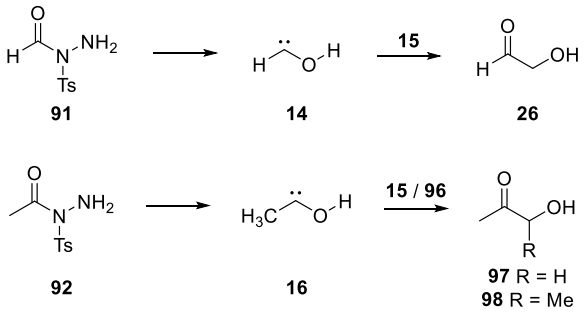

Scheme 15. Extended pool of trapping agents for a broader range of hydroxyketones.

1.5.2 Chalcogen-radicals

During this thesis we generated and spectroscopically characterized telluryl-radicals and studied their reaction with molecular oxygen by matrix isolation IR and UV/Vis spectroscopy and supported the findings with DFT-calculations. We provide the first spectroscopic data of phenyltelluryl-radical (**63**) and the generation of the new molecule phenyltelluroyl-radical. The generation of **63** offers the possibility to study the properties of this molecule and the reaction with molecular oxygen which was unknown before. During the reaction, the novel phenyltelluro hyperoxy radical formed. Photoirradiation at $\lambda = 436$ nm leads to the thermodynamically more

stable by 21.9 kcal mol^{-1} phenyltelluroyl radical. A homodesmotic equation computed at the B3LYP/def2-QZVPP level of theory also demonstrates relatively high stability comparable with benzyl radical.[178] Following this project, we also generated and spectroscopically characterized vinyltelluryl-radical (**86**) as the parent radical of phenyltelluryl-radical using the same strategy. The stability of **86** is reflected by the low BDE of 47.2 kcal mol^{-1} of the Te-Te bond of the dimeric precursor. According to NRT analysis, the spin density is mainly located at the tellurium atom similar to **63**. In comparison to **63**, doping the matrix with molecular triplet oxygen leads to the formation of vinyltelluryl hyperoxy radical. The reaction also goes further by photoirradiation with λ = 523 nm towards vinyltelluroyl radical.[194] Knowledge of the properties of these radicals provides valuable insights into the mechanism of the formation and their oxygen reactions.

This project is expandable towards vinylthiyl- (**100**) and vinylselenyl-radical (**102**). While **100** was spectroscopically observed,[196] **102** is unkown. While **102** is achievable over a similar precursor like **86**, **100** needs a different strategy using **99** and eliminating ethene. Both compounds help to better understand the properties and reactivity of these type of radicals (Scheme 16).

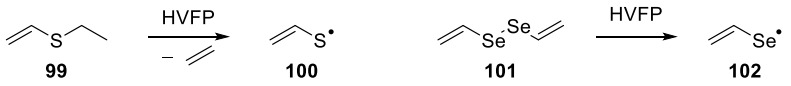

Scheme 16. Generation of vinylthiyl- **100** and vinylselenyl-radical **102**.

1.5.3 Chemistry of high-energy tautomers

As side projects, we were working on enols as high-energy tautomers of prebiotic important molecules. Enols **35** – **37** are recently reported in *Angew. Chem. Int. Ed.*[82,84] and *Chem. Sci.*[85] and are prebiotic key molecules. These enols can store energy in form of a tautomer which is important for reactions in outer space with temperatures around absolute zero. Enol **35** is suggested to contribute to the formation of sugars (pentoses in this case) in early Earth environments.[197] The tautomer of **36** – glycolic acid – is found in sugar-rich plants and meteorites and is with other polyols and carboxylic acids relevant to glycolysis.[75,198–200] Finally, reported enol **37** is suggested as a key intermediate for acetamide.[201]

1.6 Bibliography

[1] P. R. Schreiner, *J. Am. Chem. Soc.,* **2017**, *139*, 15276–15283.

[2] P. R. Schreiner, *Trends Chem.,* **2020**, *2*, 980–989.

[3] P. R. Schreiner, H. P. Reisenauer, F. C. Pickard Iv, A. C. Simmonett, W. D. Allen, E. Mátyus, A. G. Császár, *Nature,* **2008**, *453*, 906–909.

[4] A. Mardyukov, P. R. Schreiner, *Acc. Chem. Res.,* **2018**, *51*, 475–483.

[5] H. P. Reisenauer, J. Romański, G. Mlostoń, P. R. Schreiner, *Chem. Commun.,* **2015**, *51*, 10022–10025.

[6] L. Wang, Z. Wu, B. Lu, A. K. Eckhardt, P. R. Schreiner, T. Trabelsi, J. S. Francisco, Q. Yao, C. Xie, H. Guo, X. Zeng, *J. Chem. Phys.,* **2020**, *153*, 094303.

[7] Z. Wu, J. Xu, G. Deng, X. Chu, L. Sokolenko, T. Trabelsi, J. S. Francisco, A. K. Eckhardt, P. R. Schreiner, X. Zeng, *Chem. Eur. J.,* **2018**, *24*, 1505–1508.

[8] H. P. Reisenauer, P. R. Schreiner, J. Romanski, G. Mloston, *J. Phys. Chem. A,* **2015**, *119*, 2211–2216.

[9] H. P. Reisenauer, J. Romański, G. Mlostoń, P. R. Schreiner, *Chem. Commun.,* **2013**, *49*, 9467–9469.

[10] D. Gerbig, B. Bernhardt, R. C. Wende, P. R. Schreiner, *J. Phys. Chem. A,* **2020**, *124*, 2014–2018.

[11] A. Mardyukov, Y. A. Tsegaw, W. Sander, P. R. Schreiner, *Phys. Chem. Chem. Phys.* **2017**, *19*, 27384–27388.

[12] A. Mardyukov, F. Keul, P. R. Schreiner, *J. Phys. Chem. A,* **2019**, *123*, 4937–4941.

[13] IUPAC. Compendium of Chemical Terminology, 2nd ed. (the "Gold Book"). Compiled by A. D. McNaught and A. Wilkinson. Blackwell Scientific Publications, Oxford (1997). Online version (2019-) created by S. J. Chalk. ISBN 0-9678550-9-8

[14] A. Butlerow, *Justus Liebigs Ann. Chem.,* **1861**, *120*, 356–356.

[15] J. U. Nef, *Justus Liebigs Ann. Chem.,* **1892**, *270*, 267–335.

[16] J. U. Nef, *Justus Liebigs Ann. Chem.,* **1894**, *280*, 291–342.

[17] J. U. Nef, *Justus Liebigs Ann. Chem.,* **1895**, *287*, 265–359.

[18] E. Buchner, Th. Curtius, *Ber. Dtsch. Chem. Ges.,* **1885**, *18*, 2377–2379.

[19] H. Staudinger, O. Kupfer, *Ber. Dtsch. Chem. Ges.,* **1912**, *45*, 501–509.

[20] G. Herzberg, J. Shoosmith, *Nature* **1959**, *183*, 1801–1802.

[21] H. G, *Proc. R. Soc. Lon. Ser-A,* **1961**, *262*, 291–317.

[22] J. M. Foster, S. F. Boys, *Rev. Mod. Phys.,* **1960**, *32*, 305–307.

[23] P. C. H. Jordan, H. C. Longuet Higgins, *Mol. Phys.,* **1962**, *5*, 121–138.

[24] J. A. Pople, G. A. Segal, *J. Chem. Phys.,* **1966**, *44*, 3289–3296.

[25] J. F. Harrison, L. C. Allen, *J. Am. Chem. Soc.,* **1969**, *91*, 807–823.

[26] C. F. Bender, H. F. Schaefer, *J. Am. Chem. Soc.,* **1970**, *92*, 4984–4985.

[27] E. Wasserman, W. A. Yager, V. J. Kuck, *Chem. Phys. Lett.,* **1970**, *7*, 409–413.

[28] P. Jensen, P. R. Bunker, A. R. Hoy, *J. Chem. Phys.,* **1982**, *77*, 5370–5374.

[29] C. C. Hayden, D. M. Neumark, K. Shobatake, R. K. Sparks, Y. T. Lee, *J. Chem. Phys.,* **1982**, *76*, 3607–3613.

[30] W. R. Bamford, T. S. Stevens, *J. Chem. Soc.,* **1952**, 4684–4685.

[31] A. Geuther, *Justus Liebigs. Ann. Chem.,* **1862**, *123*, 121–122.

[32] J. Hine, *J. Am. Chem. Soc.,* **1950**, *72*, 2438–2445.

[33] W. von E. Doering, A. K. Hoffmann, *J. Am. Chem. Soc.,* **1954**, *76*, 6162–6165.

[34] B. A. Levi, R. W. Taft, W. J. Hehre, *J. Am. Chem. Soc.,* **1977**, *99*, 8454–8455.

[35] E. C. Ashby, A. K. Deshpande, F. Doctorovich, *J. Org. Chem.,* **1993**, *58*, 4205–4206.

[36] W. Braun, A. M. Bass, M. Pilling, M, *J. Chem. Phys.* **1970**, *52*, 5131–5143.

[37] W. Sander, G. Bucher, S. Wierlacher, *Chem. Rev.,* **1993**, *93*, 1583–1621.

[38] D. Bourissou, O. Guerret, F. P. Gabbaï, G. Bertrand, **2000**, *100,* 39–92.

[39] D. Bethell, *Adv. Phys. Org. Chem.,* **1969**, *7*, 153–209.

[40] H. P. Reisenauer, G. Maier, A. Riemann, R. W. Hoffmann, *Angew. Chem. Int. Ed.,* **1984**, *23*, 641–641.

[41] P. Thaddeus, J. M. Vrtilek, C. A. Gottlieb, *Astrophys. J.,* **1985**, *299*, L63–L66.

[42] C. A. Nixon, A. E. Thelen, M. A. Cordiner, Z. Kisiel, S. B. Charnley, E. M. Molter, J. Serigano, P. G. J. Irwin, N. A. Teanby, Y.-J. Kuan, *Astron. J.,* **2020**, *160*, 205.

[43] G. Maier, H. P. Reisenauer, W. Schwab, P. Carsky, B. A. Jr. Hess, L. J. Sshaad, *J. Am. Chem. Soc.,* **1987**, *18*, 5183–5188.

[44] G. Maier, H. P. Reisenauer, W. Schwab, P. Čársky, V. Špirko, B. A. Hess, L. J. Schaad, *J. Chem. Phys.,* **1989**, *91*, 4763–4773.

[45] G. Maier, H. P. Reisenauer, M. Cibulka, *Angew. Chem. Int. Ed.,* **1999**, *38*, 105–108.

[46] K. P. Zeller, *Tetrahedron Lett.,* **1977**, *18*, 707–708.

[47] J. P. Toscano, M. S. Platz, V. Nikolaev, Y. Cao, M. B. Zimmt, *J. Am. Chem. Soc.,* **1996**, *118*, 3527–3528.

[48] M. Ohishi, H. Suzuki, S.-I. Ishikawa, C. Yamada, H. Kanamori, W. M. Irvine, R. D. Brown, P. D. Godfrey, N. Kaifu, H. Suzuki, *Astrophys. J.,* **1991**, *380*, L39–L42.

[49] S. Saito, K. Kawaguchi, M. Ohishi, H. Suzuki, N. Kaifu, *Astrophys. J.,* **1987**, *317*, L115–L119.

[50] E. C. C. Baly, I. M. Heilbron, W. F. Barker, *J. Chem. Soc., Trans.,* **1921**, *119*, 1025–1035.

[51] R. R. Lucchese, H. F. Schaefer, *J. Am. Chem. Soc.,* **1978**, *100*, 298–299.

[52] M. J. H. Kemper, J. M. F. van Dijk, H. M. Buck, *J. Am. Chem. Soc.,* **1978**, *100*, 7841–7846.

[53] J. D. Goddard, H. F. Schaefer, *J. Chem. Phys.,* **1979**, *70*, 5117–5134.

[54] M. A. Hoffmann, H. F. Schaefer, *Astrophys. J.,* **1981**, *249*, 563–565.

[55] D. L. Reid, J. Hernández-Trujillo, J. Warkentin, *J. Phys. Chem. A,* **2000**, *104*, 3398–3405.

[56] C.-F. Pau, W. J. Hehre, *J. Phys. Chem.* **1982**, *86*, 1252–1253.

[57] P. R. Schreiner, H. P. Reisenauer, D. Ley, D. Gerbig, C. H. Wu, W. D. Allen, *Science,* **2011**, *332*, 1300–1303.

[58] D. Ley, D. Gerbig, P. R. Schreiner, *Chem. Sci.,* **2013**, *4*, 677–684.

[59] B. Bernhardt, M. Ruth, A. K. Eckhardt, P. R. Schreiner, *J. Am. Chem. Soc.,* **2021**, *143*, 3741–3746.

[60] A. Mardyukov, H. Quanz, P. R. Schreiner, *Nat. Chem.,* **2017**, *9*, 71–76.

[61] A. K. Eckhardt, F. R. Erb, P. R. Schreiner, *Chem. Sci.,* **2019**, *10*, 802–808.

[62] P. R. Schreiner, H. P. Reisenauer, *Angew. Chem. – Int. Ed.,* **2008**, *47*, 7071–7074.

[63] H. Quanz, B. Bernhardt, F. R. Erb, M. A. Bartlett, W. D. Allen, P. R. Schreiner, *J. Am. Chem. Soc.,* **2020**, *142*, 19457–19461.

[64] B. Bernhardt, M. Ruth, H. P. Reisenauer, P. R. Schreiner, *J. Phys. Chem. A,* **2021**, *125*, 7023–7028.

[65] D. Gerbig, D. Ley, H. P. Reisenauer, P. R. Schreiner, *Beilstein J. Org. Chem.,* **2010**, *6*, 1061–1069.

[66] R. Breslow, *Tetrahedron Lett.,* **1959**, *1*, 22–26.

[67] A. Butlerow, *Justus Liebigs Ann. Chem.,* **1861**, *120*, 295–298.

[68] R. F. Socha, A. H. Weiss, M. M. Sakharov, *React. Kinet. Catal. Lett.,* **1980**, *14*, 119–128.

[69] D. Ritson, J. D. Sutherland, *Nat. Chem.,* **2012**, *4*, 895–899.

[70] D. J. Ritson, J. D. Sutherland, *Angew. Chem. Int. Ed.,* **2013**, *52*, 5845–5847.

[71] S. Islam, D. K. Bučar, M. W. Powner, *Nat. Chem.,* **2017**, *9*, 584–589.

[72] S. Cannizzaro, *Justus Liebigs Ann. Chem.,* **1853**, *88*, 129–130.

[73] J. M. Hollis, F. J. Lovas, P. R. Jewell, *Astrophys. J.,* **2000**, *540*, L107–L110.

[74] J. M. Hollis, S. N. Vogel, L. E. Snyder, P. R. Jewell, F. J. Lovas, *Astrophys. J.,* **2001**, *554*, L81–L85.

[75] G. Cooper, N. Kimmich, W. Belisle, J. Sarinana, K. Brabham, L. Garrel, *Nature,* **2001**, *414*, 879–883.

[76] D. T. Halfen, A. J. Apponi, N. Woolf, R. Polt, L. M. Ziurys, *Astrophys. J.,* **2006**, *639*, 237–245.

[77] A. K. Eckhardt, M. M. Linden, R. C. Wende, B. Bernhardt, P. R. Schreiner, *Nat. Chem.,* **2018**, *10*, 1141–1147.

[78] A. K. Eckhardt, R. C. Wende, P. R. Schreiner, *J. Am. Chem. Soc.,* **2018**, *140*, 12333–12336.

[79] A. K. Eckhardt, A. Bergantini, S. K. Singh, P. R. Schreiner, R. I. Kaiser, *Angew. Chem. Int. Ed.,* **2019**, *58*, 5663–5667.

[80] N. F. Kleimeier, A. K. Eckhardt, P. R. Schreiner, R. I. Kaiser, *Chem.,* **2020**, *6*, 3385–3395.

[81] B. E. Turner, A. J. Apponi, *Astrophys. J.,* **2001**, *561*, L207.

[82] A. Mardyukov, A. K. Eckhardt, P. R. Schreiner, *Angew. Chem. Int. Ed.,* **2020**, *59*, 5577–5580.

[83] N. F. Kleimeier, A. K. Eckhardt, R. I. Kaiser, *J. Am. Chem. Soc.,* **2021**, *143*, 14009–14018.

[84] A. Mardyukov, F. Keul, P. R. Schreiner, *Angew. Chem. Int. Ed.,* **2021**, *60*, 15313–15316.

[85] A. Mardyukov, F. Keul, P. R. Schreiner, *Chem. Sci.,* **2020**, *11*, 12358–12363.

[86] A. Ricardo, M. A. Carrigan, A. N. Olcott, S. A. Benner, *Science,* **2004**, *303*, 196.

[87] H.-W. Wanzlick, *Angew. Chem.,* **1962**, *74*, 129–134.

[88] A. Igau, H. Grutzmacher, A. Baceiredo, G. Bertrand, *J. Am. Chem. Soc.,* **1988**, *110*, 6463–6466.

[89] A. J. Arduengo, R. L. Harlow, M. Kline, *J. Am. Chem. Soc.,* **1991**, *113*, 361–363.

[90] D. Enders, K. Breuer, G. Raabe, J. Runsink, J. H. Teles, J. -P Melder, K. Ebel, S. Brode, *Angew. Chem. Int. Ed.,* **1995**, *34*, 1021–1023.

[91] R. Nakano, R. Jazzar, G. Bertrand, *Nat. Chem.,* **2018**, *10*, 1196–1200.

[92] A. Berkessel, S. Elfert, V. R. Yatham, J. M. Neudörfl, N. E. Schlörer, J. H. Teles, *Angew. Chem. Int. Ed.,* **2012**, *51*, 12370–12374.

[93] D. L. Cramer, S. Bera, A. Studer, *Chem. Eur. J.,* **2016**, *22*, 7403–7407.

[94] C. Guo, M. Fleige, D. Janssen-Müller, C. G. Daniliuc, F. Glorius, *Nat. Chem.,* **2015**, *7*, 842–847.

[95] D. Lonsdale, *Evid-based. Compl. Alt.,* **2006**, *3*, 49–59.

[96] S. Mizuhara, R. Tamura, H. Arata, *Proc. Jpn. Acad.,* **1951**, *27*, 302–308.

[97] R. Breslow, *J. Am. Chem. Soc.,* **1957**, *79*, 1762–1763.

[98] R. Breslow, *J. Am. Chem. Soc.,* **1958**, *80*, 3719–3726.

[99] R. Breslow, E. Mcnelis, *J. Am. Chem. Soc.,* **1959**, *81*, 3080–3082.

[100] A. Berkessel, V. R. Yatham, S. Elfert, J. M. Neudörfl, *Angew. Chem. Int. Ed.,* **2013**, *52*, 11158–11162.

[101] M. Paul, P. Sudkaow, A. Wessels, N. E. Schlörer, J. Neudörfl, A. Berkessel, *Angew. Chem. Int. Ed.,* **2018**, *57*, 8310–8315.

[102] G. C. Vougioukalakis, R. H. Grubbs, *Chem. Rev.,* **2010**, *110*, 1746–1787.

[103] Y. Dong, J. B. Matson, K. J. Edgar, *Biomacromolecules,* **2017**, *18*, 1661–1676.

[104] E. O. Fischer, A. Maasböl, *Angew. Chem. Int. Ed.,* **1964**, *3*, 580–581.

[105] E. O. Fischer, A. Maasböl, *Chem. Ber.,* **1967**, *100*, 2445–2456.

[106] E. O. Fischer, H.-J. Beck, *Angew. Chem.,* **1970**, *82*, 44–45.

[107] E. O. Fischer, K. Weiß, C. G. Kreiter, *Chem. Inform.,* **1974**, *5*, 182–183.

[108] R. Aumann, P. Hinterding, C. Krüger, R. Goddard, *J. Organomet. Chem.,* **1993**, *459*, 145–149.

[109] W. D. Wulff, D. C. Yang, *J. Am. Chem. Soc.,* **1983**, *105*, 6726–6727.

[110] M. L. Waters, W. D. Wulff, *Org. Reactions,* **2008**, 121–623.

[111] R. R. Schrock, *J. Am. Chem. Soc.,* **1974**, *96*, 6796–6797.

[112] R. Schrock, S. Rocklage, J. Wengrovius, G. Rupprecht, J. Fellmann, *J. Mol. Catal.,* **1980**, *8*, 73–83.

[113] R. R. Schrock, J. S. Murdzek, G. C. Bazan, J. Robbins, M. DiMare, M. O'Regan, *J. Am. Chem. Soc.,* **1990**, *112*, 3875–3886.

[114] S. J. Malcolmson, S. J. Meek, E. S. Sattely, R. R. Schrock, A. H. Hoveyda, *Nature,* **2008**, *456*, 933–937.

[115] F. N. Tebbe, G. W. Parshall, G. S. Reddy, *J. Am. Chem. Soc.,* **1978**, *100*, 3611–3613.

[116] G. Wittig, U. Schöllkopf, *Chem. Ber.,* **1954**, *87*, 1318–1330.

[117] P. Schwab, M. B. France, J. W. Ziller, R. H. Grubbs, *Angew. Chem. Int. Ed.,* **1995**, *34*, 2039–2041.

[118] P. Schwab, R. H. Grubbs, J. W. Ziller, *J. Am. Chem. Soc.,* **1996**, *118*, 100–110.

[119] M. Scholl, S. Ding, C. W. Lee, R. H. Grubbs, *Org. Lett.,* **1999**, *1*, 953–956.

[120] J. S. Kingsbury, J. P. A. Harrity, P. J. Bonitatebus, A. H. Hoveyda, *J. Am. Chem. Soc.,* **1999**, *121*, 791–799.

[121] S. B. Garber, J. S. Kingsbury, B. L. Gray, A. H. Hoveyda, *J. Am. Chem. Soc.,* **2000**, *122*, 8168–8179.

[122] J. S. McFadyen, T. S. Stevens, *J. Chem. Soc.,* **1936**, 584–587.

[123] H. Babad, W. Herbert, A. W. Stiles, *Tetrahedron Lett.,* **1966**, *7*, 2927–2931.

[124] Y. Iwai, T. Ozaki, R. Takita, M. Uchiyama, J. Shimokawa, T. Fukuyama, *Chem. Sci.,* **2013**, *4*, 1111.

[125] E. Campaigne, R. L. Thompson, J. E. Van Werth, *J. Med. Pharm. Chem.,* **1959**, *1*, 577–599.

[126] S. Matin, J. Craig, R. Chan, *J. Org. Chem.,* **1974**, *39*, 2285–2289.

[127] F. Weigend, R. Ahlrichs, *Phys. Chem. Chem. Phys.,* **2005**, *7*, 3297.

[128] J. L. Bao, D. G. Truhlar, *Chem. Soc. Rev.,* **2017**, *46*, 7548–7596.

[129] F. Keul, A. Mardyukov, P. R. Schreiner, *J. Phys. Org. Chem.,* **2022**, *35*, e4315.

[130] A. Taylor, *Biol. Trace Elem. Res.,* **1996**, *55*, 231–239.

[131] H. A. Schroeder, J. Buckman, J. J. Balassa, *J. Chronic. Dis.,* **1967**, *20*, 147–161.

[132] G. T. Morgan, H. D. K. Drew, *J. Chem. Soc., Trans.,* **1922**, *121*, 922–940.

[133] M. J. Dabdoub, V. B. Dabdoub, J. P. Marino, *Tetrahedron Lett.,* **2000**, *41*, 437–440.

[134] D. H. R. Barton, M. Ramesh, *J. Am. Chem. Soc.,* **1990**, *112*, 891–892.

[135] G. T. Morgan, E. A. Cooper, A. W. Burtt, *Biochem. J.,* **1923**, *17*, 30–33.

[136] A. Fleming, *J. Pathol. Bacteriol.,* **1932**, *35*, 831–842.

[137] A. Fleming, M. Y. Young, *J. Pathol. Bacteriol.,* **1940**, *51*, 29–35.

[138] E. Zonaro, S. Lampis, R. J. Turner, S. Junaid, G. Vallini, *Front. Microbiol.,* **2015**, *6*, 584.

[139] M. Daniel-Hoffmann, M. Albeck, B. Sredni, Y. Nitzan, *Arch. Microbiol.,* **2009**, *191*, 631–638.

[140] R. K. Matharu, Z. Charani, L. Ciric, U. E. Illangakoon, M. Edirisinghe, *J. Appl. Polym. Sci.,* **2018**, *135*, 46368.

[141] A. B. Sabti, A. A. Al-Fregi, M. Y. Yousif, *Molecules,* **2020**, *25*, 3439.

[142] B. Sredni, T. Tichler, A. Shani, R. Catane, B. Kaufman, G. Strassmann, M. Albeck, Y. Kalechman, *J. Natl. Cancer I.,* **1996**, *88*, 1276–1284.

[143] B. Sredni, R.-H. Xu, M. Albeck, U. Gafter, R. Gal, A. Shani, T. Tichler, J. Shapira, I. Bruderman, R. Catane, B. Kaufman, J. K. Whisnant, K. L. Mettinger, Y. Kalechman, *Int. J. Cancer,* **1996**, *65*, 97–103.

[144] Y. Kalechman, U. Gafter, J. P. Da, M. Albeck, D. Alarcon-Segovia, B. Sredni, *J. Immunol.,* **1997**, *159*, 2658–67.

[145] Y. Kalechman, U. Gafter, T. Weinstein, A. Chagnac, I. Freidkin, A. Tobar, M. Albeck, B. Sredni, *J. Biol. Chem.,* **2004**, *279*, 24724–24732.

[146] B. Sredni, M. Weil, G. Khomenok, I. Lebenthal, S. Teitz, Y. Mardor, Z. Ram, A. Orenstein, A. Kershenovich, S. Michowiz, Y. I. Cohen, Z. H. Rappaport, I. Freidkin, M. Albeck, D. L. Longo, Y. Kalechman, *Cancer Res.,* **2004**, *64*, 1843–1852.

[147] L. Engman, N. Al-Maharik, M. McNaughton, A. Birmingham, G. Powis, *Bioorg. Med. Chem.,* **2003**, *11*, 5091–5100.

[148] D. S. Ávila, P. Gubert, A. Palma, D. Colle, D. Alves, C. W. Nogueira, J. B. T. Rocha, F. A. A. Soares, *Brain. Res. Bull.,* **2008**, *76*, 114–123.

[149] B. P. Laden, T. D. Porter, *J. Lipid. Res.,* **2001**, *42*, 235–240.

[150] H. Suzuki, T. Nakamura, *Synthesis,* **1992**, *1992*, 549–551.

[151] J. Li, P. Lue, X.-J. Zhou, *Synthesis,* **1992**, *1992*, 281–283.

[152] L. B. Han, K. I. Ishihara, N. Kambe, A. Ogawa, I. Ryu, N. Sonoda, *J. Am. Chem. Soc.* **1992**, *114*, 7591–7592.

[153] L. B. Han, K. I. Ishihara, N. Kambei, A. Ogawa, N. Sonoda, *Phosphorus Sulfur,* **1992**, *67*, 243–246.

[154] F. K. Zinn, V. E. Righi, S. C. Luque, H. B. Formiga, J. V. Comasseto, *Tetrahedron Lett.,* **2002**, *43*, 1625–1628.

[155] L. Engman, J. Persson, *Synth. Commun.,* **1993**, *23*, 445–458.

[156] X. Jia, P. Jin, Y. Zhang, X. Zhou, *Synth. Commun.,* **1995**, *25*, 253–258.

[157] H. Suzuki, T. Nakamura, *J. Org. Chem.,* **1993**, *58*, 241–244.

[158] G. Blay, L. Cardona, B. García, L. Lahoz, JoséR. Pedro, *Tetrahedron,* **1996**, *52*, 8611–8618.

[159] A. S. Pepito, D. C. Dittmer, *J. Org. Chem*., **1997**, *62*, 7920–7925.

[160] H. Suzuki, S. Kawato, A. Nasu, *Bull. Chem. Soc. Jpn.,* **1992**, *65*, 626–627.

[161] X. Huang, L. Xie, H. Wu, *J. Org. Chem.,* **1988**, *53*, 4862–4864.

[162] Y. Z. Huang, Y. Tang, Z. L. Zhou, *Tetrahedron,* **1998**, *54*, 1667–1690.

[163] L. L. Shi, Z. L. Zhou, Y. Z. Huang, *Tetrahedron Lett.,* **1990**, *31*, 4173–4174.

[164] T. Hiiro, N. Kambe, A. Ogawa, N. Miyoshi, S. Murai, N. Sonoda, *Angew. Chem. Int. Ed.,* **1987**, *26*, 1187–1188.

[165] T. Kanda, S. Kato, T. Sugino, N. Kambe, N. Sonoda, *J. Organomet. Chem.,* **1994**, *473*, 71–83.

[166] S.-K. Kang, S.-W. Lee, H.-C. Ryu, *Chem. Commun.,* **1999**, *20*, 2117–2118.

[167] A. E. Okoronkwo, B. Godoi, R. F. Schumacher, J. Sebastião, S. Neto, C. Luchese, M. Prigol, C. W. Nogueira, G. Zeni, *Tetrahedron Lett.,* **2008**, *50*, 909–915.

[168] A. L. Braga, D. S. Lüdtke, F. Vargas, R. K. Donato, C. C. Silveira, H. A. Stefani, G. Zeni, *Tetrahedron Lett.,* **2003**, *44*, 1779–1781.

[169] R. Cella, R. L. O. R. Cunha, A. E. S. Reis, D. C. Pimenta, C. F. Klitzke, H. A. Stefani, *J. Org. Chem.,* **2006**, *71*, 244–250.

[170] D. H. R. Barton, S. D. Géro, Q. S. Béatrice, M. Samadi, C. Vincent, *Tetrahedron,* **1991**, *47*, 9383–9392.

[171] D. H. R. Barton, P. I. Dalko, S. D. Géro, *Tetrahedron Lett.,* **1991**, *32*, 4713–4716.

[172] D. Crich, C. Chen, J. T. Hwang, H. Yuan, A. Papadatos, R. I. Walter, *J. Am. Chem. Soc.* **1994**, *116*, 8937–8951.

[173] S. Yamago, H. Miyazoe, R. Goto, J. Yoshida, *Tetrahedron Lett.,* **1999**, *40*, 2347–2350.

[174] S. Yamago, H. Miyazoe, T. Sawazaki, R. Goto, J. I. Yoshida, *Tetrahedron Lett.,* **2000**, *41*, 7517–7520.

[175] S. Yamago, H. Miyazoe, R. Goto, M. Hashidume, T. Sawazaki, J. Yoshida, *J. Am. Chem. Soc.,* **2001**, *123*, 3697–3705.

[176] S. Yamago, M. Miyoshi, H. Miyazoe, J. Yoshida, *Angew. Chem. Int. Ed.,* **2002**, *41*, 1407–1409.

[177] H. Miyazoe, S. Yamago, J. I. Yoshida, *Angew. Chem. Int. Ed.,* **2000**, *39*, 3669–3671.

[178] F. Keul, A. Mardyukov, P. R. Schreiner, *Phys. Chem. Chem. Phys.* **2019**, *21*, 25797–25801.

[179] S. Yamago, K. Iida, J. I. Yoshida, *J. Am. Chem. Soc.,* **2002**, *124*, 2874–2875.

[180] S. Yamago, K. Iida, J. ichi Yoshida, *J. Am. Chem. Soc.,* **2002**, *124*, 13666–13667.

[181] S. Yamago, K. Iida, M. Nakajima, J. I. Yoshida, *Macromolecules,* **2003**, *36*, 3793–3796.

[182] E. Mishima, S. Yamago, *Macromol. Rapid. Commun.,* **2011**, *32*, 893–898.

[183] E. Mishima, T. Tamura, S. Yamago, *Macromolecules,* **2012**, *45*, 2989–2994.

[184] E. Mishima, T. Tamura, S. Yamago, *Macromolecules,* **2012**, *45*, 8998–9003.

[185] E. Mishima, S. Yamago, *J. Polym. Sci. Pol. Chem.,* **2012**, *50*, 2254–2264.

[186] W. Fan, S. Yamago, *Angew. Chem. Int. Ed.,* **2019**, *58*, 7113–7116.

[187] Y. Lu, S. Yamago, *Angew. Chem. Int. Ed.,* **2019**, *58*, 3952–3956.

[188] S. I. Yusa, S. Yamago, M. Sugahara, S. Morikawa, T. Yamamoto, Y. Morishima, *Macromolecules,* **2007**, *40*, 5907–5915.

[189] J. Hasegawa, K. Kanamori, K. Nakanishi, T. Hanada, S. Yamago, *Macromol. Rapid. Commun.,* **2009**, *30*, 986–990.

[190] J. Hasegawa, K. Kanamori, K. Nakanishi, T. Hanada, S. Yamago, *Macromolecules,* **2009**, *42*, 1270–1277.

[191] G. Hasegawa, K. Kanamori, K. Nakanishi, S. Yamago, *Polymer,* **2011**, *52*, 4644–4647.

[192] S. Yamago, Y. Yahata, K. Nakanishi, S. Konishi, E. Kayahara, A. Nomura, A. Goto, Y. Tsujii, *Macromolecules,* **2013**, *46*, 6777–6785.

[193] Y. Lu, T. Nemoto, M. Tosaka, S. Yamago, *Nat, Commun.,* **2017**, *8*, 1–8.

[194] F. Keul, A. Mardyukov, *Phys. Chem. Chem. Phys.,* **2022**, *24*, 15129–15134.

[195] D. Gerbig, H. P. Reisenauer, C. H. Wu, D. Ley, W. D. Allen, P. R. Schreiner, *J. Am. Chem. Soc.,* **2010**, *132*, 7273–7275.

[196] M. Nakajima, A. Miyoshi, Y. Sumiyoshi, Y. Endo, *J. Chem. Phys.,* **2007**, *126*, 044307.

[197] A. Ricardo, M. A. Carrigan, A. N. Olcott, S. A. Benner, *Science,* **2004**, *303*, 196.

[198] Y. Kebukawa, A. L. David Kilcoyne, G. D. Cody, *Astrophys. J.,* **2013**, *771*, 19.

[199] A. A. Monroe, S. Pizzarello, *Geochim. Cosmochim. Acta,* **2011**, *75*, 7585–7595.

[200] K. B. Muchowska, S. J. Varma, J. Moran, *Nature,* **2019**, *569*, 104–107.

[201] L. Foo, A. Surányi, A. Guljas, M. Szőri, J. J. Villar, B. Viskolcz, I. G. Csizmadia, A. Rágyanszki, B. Fiser, *Mol. Astrophys.,* **2018**, *13*, 1–5.

2 Publications

2.1 Generation and Reactivity of Phenylhydroxycarbenes in Solution

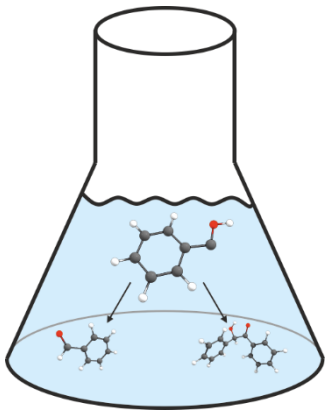

Abstract. We provide evidence for the first successful generation of phenylhydroxycarbene and 4-trifluoromethylphenylhydroxycarbene in solution. The carbene tautomers of the corresponding benzaldehyde derivatives had been prepared under cryogenic matrix-isolation conditions before but their reactivity, apart from a prototypical quantum mechanical tunneling [1,2]-H-shift reaction, had not been studied. Here our strategy is to employ suitable carbene precursors for the McFadyen–Stevens reaction, to generate the parent and the *para*-CF_3-substituted phenylhydroxycarbenes, and to react them with benzaldehyde or acetone in a highly facile, allowed six-electron carbonyl-ene reaction toward the corresponding α-hydroxy ketones. Our findings are supported by computations at the DLPNO-CCSD(T)/cc-pVQZ//B3LYP/def2-TZVP level of theory.

Reference. Generation and Reactivity of Phenylhydroxycarbene in Solution, F. Keul, A. Mardyukov, Peter R. Schreiner, *J. Phys. Org. Chem.*, **2022**, *35*, e4315, DOI: 10.1002/poc.4315.

Check for updates

Received: 9 December 2021 | Accepted: 18 December 2021

DOI: 10.1002/poc.4315

RESEARCH ARTICLE

Journal of Physical Organic Chemistry WILEY

Generation and reactivity of phenylhydroxycarbenes in solution

Felix Keul | **Artur Mardyukov** | **Peter R. Schreiner**

Institute of Organic Chemistry, Justus Liebig University, Giessen, Germany

Correspondence
Peter R. Schreiner, Institute of Organic Chemistry, Justus Liebig University, Heinrich-Buff-Ring 17, 35392 Giessen, Germany.
Email: prs@uni-giessen.de

Funding information
Volkswagen Foundation, Grant/Award Number: What is Life grant 92 748; Justus Liebig Universitaet Giessen

Abstract

We provide evidence for the first successful generation of phenylhydroxycarbene and 4-trifluoromethylphenylhydroxycarbene in solution. The carbene tautomers of the corresponding benzaldehyde derivatives had been prepared under cryogenic matrix-isolation conditions before but their reactivity, apart from a prototypical quantum mechanical tunneling [1,2]-H-shift reaction, had not been studied. Here our strategy is to employ suitable carbene precursors for the McFadyen–Stevens reaction, to generate the parent and the *para*-CF_3-substituted phenylhydroxycarbenes, and to react them with benzaldehyde or acetone in a highly facile, allowed six-electron carbonyl-ene reaction toward the corresponding α-hydroxy ketones. Our findings are supported by computations at the DLPNO-CCSD(T)/cc-pVQZ//B3LYP/def2-TZVP level of theory.

KEYWORDS

carbene, carbonyl-ene reaction, tunneling

1 | INTRODUCTION

Even though hydroxymethylene (hydroxycarbene, H—C̈—OH) had been implicated in the photocatalytic formation of carbohydrates as early as 1921[1] and was recognized as the high-energy and highly reactive tautomer of formaldehyde,[2–6] it was first prepared and characterized under matrix isolation conditions at cryogenic temperatures only in 2008.[7] Parent hydroxymethylene undergoes a tunneling reaction *via* [1,2]-H-shift to formaldehyde with a half-life of 2 h. With the analogously prepared methylhydroxycarbene, the kinetically favored reaction to the corresponding enol does not occur, leading to the new reaction paradigm of *tunneling control* where the thermodynamically favored product forms preferentially through a quantum mechanical tunneling reaction.[8–10] Hydroxymethylene and the entire hydroxycarbene family now can routinely be prepared through CO_2 extrusion from α-keto carboxylic acids, and hydroxycarbenes undergo tunneling with half-lives typically in the range of several hours.[8,10–12] The behavior of phenylhydroxycarbene (**1**) and some of its derivatives has been well studied.[11–13] In contrast to other phenyl-substituted carbenes like phenylcarbene and phenylchlorocarbene, it does not undergo a ring expansion reaction.[14–16] Under cryogenic conditions **1** shows H-tunneling to benzaldehyde with a measured first-order-decay half-life of $\tau = 2–3$ h at cryogenic temperatures.[12] In subsequent studies, (*o*-methoxyphenyl)glyoxylic acid was used to generate *o*-methoxyphenylhydroxycarbene,[11] which, however, was not observed. Instead, a C—H-bond insertion to

This is an open access article under the terms of the Creative Commons Attribution-NonCommercial-NoDerivs License, which permits use and distribution in any medium, provided the original work is properly cited, the use is non-commercial and no modifications or adaptations are made.
© 2022 The Authors. *Journal of Physical Organic Chemistry* published by John Wiley & Sons Ltd.

2,3-dihydrobenzofuran-3-ol took place. Alternative hydroxycarbene reactivity was reported for the reactions toward sugar formation. In a bimolecular reaction several hydroxycarbene derivatives have been shown to react in a nearly barrierless carbonyl-ene reaction with aldehydes and ketones.[17] This is made possible through an allowed, highly facile (extremely low barrier) six-electron carbonyl-ene reaction,[18] which is mechanistically close to the Alder-ene reaction,[19,20] through five-membered ring transition structures where the carbene lone pair replaces the olefinic double bond of the Alder-ene reaction.

The standard procedure for the generation of hydroxycarbenes *via* pyrolysis of α-keto carboxylic acids cannot be transferred into solution for two reasons. First, the free carbene will very rapidly be protonated by the acidic starting materials. Second, the activation barrier for CO_2 extrusion is too high (∼ 40 kcal mol^{-1}) for the temperatures to be conveniently reached with typical organic solvents.

An alternative may be offered by the long known McFadyen-Stevens reaction that converts acids to aldehydes.[21] For example, it has been reported that benzenesulphonacyl hydrazide (**3**) derived from benzoic acid undergoes N_2 extrusion at 160 °C to give benzaldehyde (**5**) upon treatment with alkaline carbonates (Scheme 1).[21] One of the first postulated mechanism was a one-step elimination through acyldiimide intermediate **4**.[22,25] In 1974, Matin *et al.* reinvestigated the reaction and were first to suggest **1** as an intermediate.[23] As the McFadyen–Stevens reaction originally needs harsh conditions, Iwai *et al.* introduced derivatives of **2** as more reactive starting materials, which allows the use of weak bases (e.g., imidazole) and much lower temperatures (55 °C).[24] Mechanistic studies imply the intermediacy of **1** so that we deemed **2** as a suitable precursor for the generation of **1** and related hydroxycarbenes in solution.

Here we provide evidence for the intermediacy of **1** in solution through using it as a reactant for bimolecular reactions that are indicative for the involvement of a carbene. We thereby draw on nearly barrierless and therefore fast, diffusion-controlled carbonyl-ene reactions of **1** with aldehydes or ketones yielding α-hydroxyketones (acetoins).[17]

2 | RESULTS AND DISCUSSION

Because we cannot directly detect **1** in solution due to its high reactivity, we decided to trap it through the established carbonyl-ene reaction.[18] We first used the Fukuyama protocol employing imidazole/TMS-imidazole as bases in toluene[24] with the hope that in situ generated **1** reacts with **5** that forms during the reaction. To increase the probability of trapping **1**, we added a large

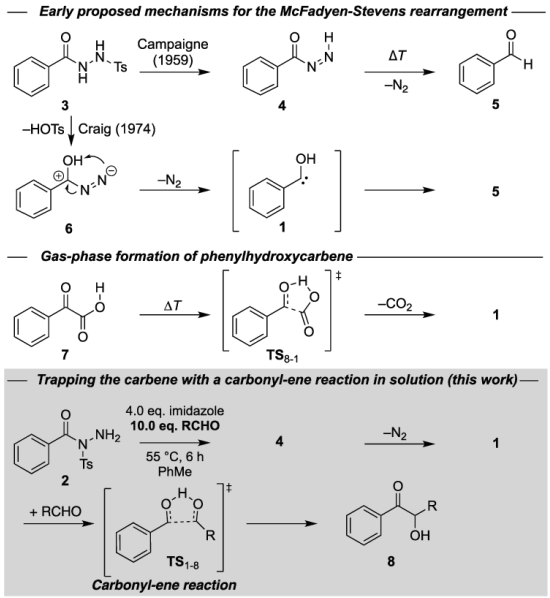

SCHEME 1 Early proposals of the mechanism of McFadyen–Stevens reaction.[22,23] Generation of phenylhydroxycarbene (**1**) in the gas-phase[12] and trapping **1** in solution[24]

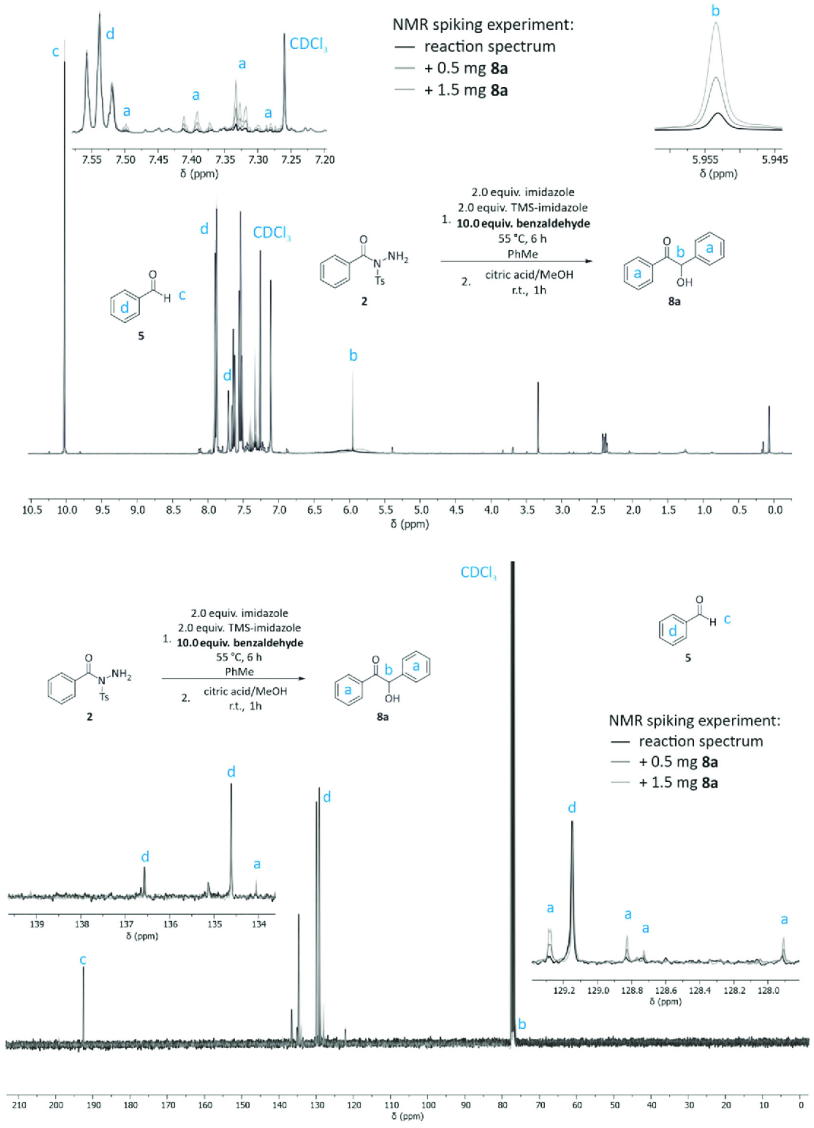

FIGURE 1 Top: nuclear magnetic resonance (NMR) spectra of benzoin derived from the reactions of precursor **2** *via* the reaction of intermediate **1** with benzaldehyde in solution. The ^{1}H-NMR spectrum (400 MHz, $CDCl_3$) was recorded after acidic work up of the resulting reaction mixture performing a McFadyen–Stevens reaction and subsequent spiking by adding 0.5 and 1.5 mg of pure **8a**. Bottom: NMR spectra of benzoin derived from the reactions of precursor **2** *via* the reaction of intermediate **1** with benzaldehyde in solution. The ^{13}C-NMR spectrum (100 MHz, $CDCl_3$) was recorded after acidic work up of the resulting reaction mixture performing a McFadyen-Stevens reaction and subsequent spiking by adding 0.5 and 1.5 mg of pure **8a**

excess of 10 equiv. of **5** to the reaction mixture. After work up with citric acid to neutralize and remove the bases, we obtained a yellow oil. The nuclear magnetic resonance (NMR) spectrum (Figure 1) shows full conversion of **2** and the spectral signature of benzoin **8a** (R = Ph). The characteristic peak of **8a** in the ^{1}H-NMR spectrum is the singlet at 5.96 ppm (b) for the *H*COH group. Even though the aromatic region is crowded due to the presence of **5**, the multiplets at 7.93–7.26 ppm (a) can be assigned to **8a**, as evident from spiking experiments with externally prepared authentic **8a** (Figure 1). The strong singlet at 10.03 ppm (d) belongs to the carbonyl proton of remaining **5**, as do the multiplets at 7.91–7.51 ppm (c). In the ^{13}C-NMR spectrum, we are also able to identify key signals belonging to **8a** with exception of all quarternary and the hydroxyl carbon atoms (Figure 1). Note that the potential background reaction *without* **2** did not produce benzoin (Figure S1). We also did not observe the formation of 1,2-diphenylethanol as the C—H-bond insertion product of toluene and **1**. Cannizzaro products typical for McFadyen–Stevens reactions were also not detected.[26,27]

For further proof of the formation of **1** in solution, we used acetone (**9**) as a reactant to perform a cross-reaction to that should produce 2-hydroxy-2-methylpropiophenone (**8b**, R=CH_3) using the same conditions as before. Integration of the ^{1}H-NMR spectrum indicates the formation of **5** as the McFadyen–Stevens product and **8b**, which is evident from the multiplets at 8.03–7.51 (overlap with **5**) and 7.50–7.43 ppm (a). The broad singlet at 2.75 ppm corresponds to the OH function (Figure S2). During spiking with pure **8b**, the singlet shifts to low field because of concentration changes. The characteristic signal of **8b** is the singlet of the methyl groups at 1.64 ppm (c). The formation of **8a** as a side product of **1** reacting with **9** was not observed due to the small amount of **5**. In the ^{13}C-NMR spectrum (Figure S3) the peaks at 133.9, 133.1, 129.8, and 128.6 ppm (b) can be assigned to aromatic carbons of **8**; the methyl groups appear characteristically at 28.6 ppm (d). The carbonyl carbon (a) and *C*OH (c) are not observed without spiking (Figure S3) due to their low intensity. Peaks at 134.6, 129.9, and 129.2 were assigned to **5** *via* comparison with pure **5** (Figure S3).

To avoid the formation of phenylsiloxycarbene as a potential intermediate, we simplified the reaction conditions by not using TMS-imidazole. Instead, we used a large excess (4.00 equiv.) of imidazole as the base and extended the reaction time to 16 h at 55 °C. Under these conditions, we also obtained **8a** with an NMR yield of 6% and **8b** with 15%. The yields were determined with *p*-nitrobenzaldehyde as the internal standard.

In a cross-reaction with another phenylhydroxycarbene derivative, we used the para-substituted trifluoromethyl precursor **10** under the simplified reaction conditions (Scheme 2). We attempted to react **11** with 4-trifluoromethylbenzaldehyde (**12**) but did not observe the benzoin derivative **13a**. The electron-withdrawing group of **12** apparently led to a significantly decreased reactivity of the carbonyl moiety.

Success was achieved with **9** as reactant for trapping **11**, leading to hydroxyketone **13b**. Besides the formation of **12** as a side product, we observed in ^{1}H-NMR spectrum a singlet at 1.62 ppm, which is characteristic for the methyl groups of **13b** (NMR yield of 14%).

3 | COMPUTATIONS

To support our findings, we computed the potential energy hypersurface (PES) of the reactions above. We performed geometry optimizations at the B3LYP/def2-TZVP[28] level of theory and improved the relative energies with single point energy computations at DLPNO-CCSD(T)/cc-pVQZ.[29,30] With adding thermal corrections for 55 °C and solvation energies with the SMD-solvent model[31] with toluene as the solvent, the computed PES should capture the key features of our experiments. Starting from elimination product **4**, **1** forms *via* nitrogen extrusion through a five-membered cyclic transition structure ($\mathbf{TS}_{1-4}$) with a free activation barrier of 21.9 kcal mol^{-1} ($\Delta^{\ddagger}G_{55\,°C,\ Solv}$, DLPNO-CCSD(T)/cc-pVQZ//B3LYP/def2-TZVP level of theory—these energies are used throughout). In earlier gas-phase studies,[12] the activation barrier for CO_2 extrusion of phenylglyoxylic acid (**7**) to **1** is 36.7 kcal mol^{-1} (M06-2X/cc-pVDZ). The formation of **8a** in solution follows a concerted reaction mechanism, with **1** forming with **5** C_s-complex **1•5**, which is 0.8 kcal mol^{-1} lower in energy than **1**. This leads straight into a carbonyl-ene like five-center-six-electron transition structure $\mathbf{TS}_{\mathbf{1•5-8a}}$. After the out-of-plane

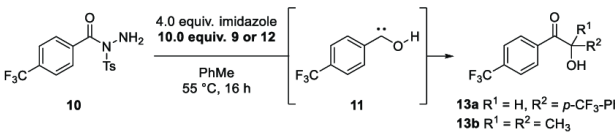

SCHEME 2 Generation of 4-trifluoromethylphenylhydroxycarbene **11** in solution and trapping reactions

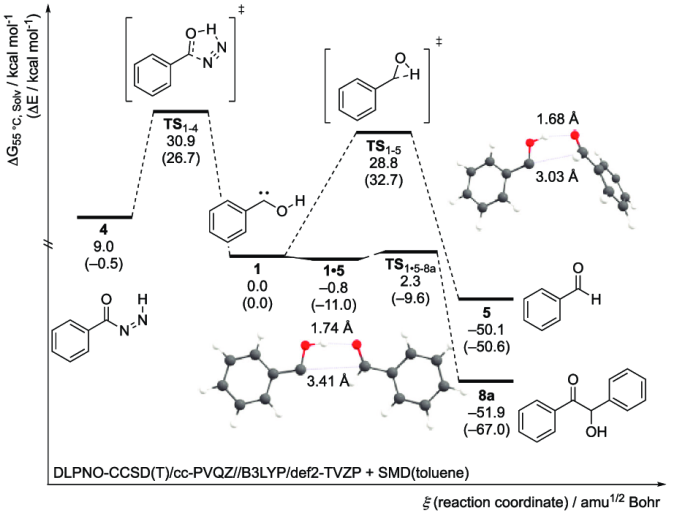

FIGURE 2 Potential energy hypersurface of nitrogen extrusion of **4** to **1** and the reaction with benzaldehyde to benzoin **8a**. Computations at the DLPNO-CCSD(T)/cc-pVQZ//B3LYP/def2-TZVP level of theory with temperature and SMD (toluene)-solvent corrections. N_2 is not depicted but included in the computations

rotation of the benzaldehyde moiety, benzoin **8a** forms (Figure 2).

Besides benzoin formation, **1** can undergo a typical [1,2]-H-shift with a barrier of 28.8 kcal mol^{-1} (*via* $\mathbf{TS_{1-5}}$) to **5** (Figure 2). To rationalize why the yields would be so low for a nearly barrierless reaction, we wondered whether the background quantum mechanical [1,2]-H-tunneling shift from **1** to **5** could effectively compete by consuming **1** at 55 °C. We anticipated that the half-life of 2.5 h of this reaction at 10 K will be significantly shortened at higher temperatures owing to vibrationally assisted tunneling[32] and an effectively thinner barrier width.[9,10] We computed the tunneling half-lives of the [1,2]-H-shift of **1** and **11** (vide infra) toward the corresponding aldehydes **5** and **12** using canonical variational theory (CVT) in conjunction with small curvature tunneling (SCT)[33] at the B3LYP/def2-TZVP level of theory. At a temperature of 55 °C the half-lives are merely $\tau = 84$ s for **1** and $\tau = 41$ ns for **11**, respectively. Hence, the low yields for the hydroxyketone products are likely due to a fast tunneling background reaction to the corresponding aldehydes.

In the cross-reaction of **1** with acetone (**9**), a transition structure could not be located, which is likely to be due to the exceedingly low barrier. The reaction proceeds directly to 2-hydroxy-2-methyl-phenylpropanone **13b** (Figure S7).

Introducing a trifluoromethyl group in *para*-position does not affect N_2 extrusion much; the activation barrier is similar to the parent case (Figure S9). The [1,2]-H-shift barrier is slightly higher than for the parent case, resulting in a longer half-life but a transition structure for this hydrogen shift could also not be located. For the formation of **13a**, the activation barrier is 5.4 kcal mol^{-1} (2.3 kcal mol^{-1} more than for **8a**). Therefore, the barrier is high enough that only the background reaction toward **5** takes places by a thermal and tunneling[1,2] H-shift.

4 | CONCLUSIONS

We used new precursors for the McFadyen–Stevens reaction to generate the hydroxycarbenes **1** and **11** in toluene solution *via* base-initiated N_2 extrusion. As the hydroxycarbene intermediates cannot be identified directly spectroscopically owing to their high reactivity and short tunneling half-lives (computed to be 84 s and 41 ns) we reacted them with benzaldehyde or acetone. The formation of their corresponding acetoins *via* a very facile, essentially barrierless carbonyl-ene is suggested as evidence for the intermediacy of the carbenes in solution. Our findings are well supported by computations at the DLPNO-CCSD(T)/cc-pVQZ level of theory.

ACKNOWLEDGMENTS

This work was supported by the Volkswagen Foundation ("What is Life" grant 92 748). We thank Markus Schauermann and Bastian Bernhardt for their support with the polyrate tunneling computations. Open Access funding enabled and organized by Projekt DEAL.

CONFLICT OF INTEREST

The authors declare no competing interests.

ORCID

Peter R. Schreiner https://orcid.org/0000-0002-3608-5515

REFERENCES

[1] E. C. C. Baly, I. M. Heilbron, W. F. Barker, *J. Chem. Soc. Trans.* **1921**, *119*, 1025.
[2] M. Kemper, J. Van Dijk, H. Buck, *J. Am. Chem. Soc.* **1978**, *100*, 7841.
[3] R. R. Lucchese, H. F. Schaefer III, *J. Am. Chem. Soc.* **1978**, *100*, 298.
[4] M. R. Hoffmann, H. F. Schaefer III, *Astrophys. J.* **1981**, *249*, 563.
[5] J. D. Goddard, H. F. Schaefer III, *J. Chem. Phys.* **1979**, *70*, 5117.
[6] D. L. Reid, J. Hernández-Trujillo, J. Warkentin, *J. Phys. Chem. A* **2000**, *104*, 3398.
[7] P. R. Schreiner, H. P. Reisenauer, F. C. Pickard IV, A. C. Simmonett, W. D. Allen, E. Matyus, A. G. Csaszar, *Nature* **2008**, *453*, 906.
[8] P. R. Schreiner, H. P. Reisenauer, D. Ley, D. Gerbig, C.-H. Wu, W. D. Allen, *Science* **2011**, *332*, 1300.
[9] P. R. Schreiner, *J. Am. Chem. Soc.* **2017**, *139*, 15276.
[10] P. R. Schreiner, *Trends Chem.* **2020**, *2*, 980.
[11] D. Gerbig, D. Ley, H. P. Reisenauer, P. R. Schreiner, *Beilstein J. Org. Chem.* **2010**, *6*, 1061.
[12] D. Gerbig, H. P. Reisenauer, C.-H. Wu, D. Ley, W. D. Allen, P. R. Schreiner, *J. Am. Chem. Soc.* **2010**, *132*, 7273.
[13] M. Schäfer, K. Peckelsen, M. Paul, J. Martens, J. Oomens, G. Berden, A. Berkessel, A. J. Meijer, *J. Am. Chem. Soc.* **2017**, *139*, 5779.
[14] P. R. West, O. L. Chapman, J. P. LeRoux, *J. Am. Chem. Soc.* **1982**, *104*, 1779.
[15] P. P. Gaspar, J.-P. Hsu, S. Chari, M. Jones Jr., *Tetrahdedron* **1985**, *41*, 1479.
[16] W. W. Sander, *Spectrochim. Acta A-M* **1987**, *43*, 637.
[17] A. K. Eckhardt, M. M. Linden, R. C. Wende, B. Bernhardt, P. R. Schreiner, *Nat. Chem.* **2018**, *10*, 1141.
[18] M. L. Clarke, M. B. France, *Tetrahdedron* **2008**, *64*, 9003.
[19] H. Hoffmann, *Angew. Chem. Int. Ed.* **1969**, *8*, 556.
[20] K. Mikami, M. Shimizu, *Chem. Rev.* **1992**, *92*, 1021.
[21] J. S. McFadyen, T. S. Stevens, *J. Chem. Soc.* **1936**, 584.
[22] E. Campaigne, R. L. Thompson, J. E. Van Werth, *J. Med. Pharm. Chem.* **1959**, *1*, 577.
[23] S. Matin, J. Craig, R. Chan, *J. Organomet. Chem.* **1974**, *39*, 2285.
[24] Y. Iwai, T. Ozaki, R. Takita, M. Uchiyama, J. Shimokawa, T. Fukuyama, *Chem. Sci.* **2013**, *4*, 1111.
[25] D. J. Cram, J. S. Bradshaw, *J. Am. Chem. Soc.* **1963**, *85*, 1108.
[26] H. Babad, W. Herbert, A. W. Stiles, *Tetrahedron Lett.* **1966**, *7*, 2927.
[27] M. Nair, H. Shechter, *J. Chem. Soc. Chem. Commun.* **1978**, 793.
[28] F. Weigend, R. Ahlrichs, *Phys. Chem. Chem. Phys.* **2005**, *7*, 3297.
[29] C. Riplinger, F. Neese, *J. Chem. Phys.* **2013**, *138*, 034106.
[30] C. Riplinger, B. Sandhoefer, A. Hansen, F. Neese, *J. Chem. Phys.* **2013**, *139*, 134101.
[31] A. V. Marenich, C. J. Cramer, D. G. Truhlar, *J. Phys. Chem. B* **2009**, *113*, 6378.
[32] M. J. Dewar, K. M. Merz, J. J. Stewart, *J. Chem. Soc. Chem. Commun.* **1985**, 166.
[33] J. L. Bao, D. G. Truhlar, *Chem. Soc. Rev.* **2017**, *46*, 7548.

SUPPORTING INFORMATION

Additional supporting information may be found in the online version of the article at the publisher's website.

How to cite this article: F. Keul, A. Mardyukov, P. R. Schreiner, *J Phys Org Chem* **2022**, e4315. https://doi.org/10.1002/poc.4315

2.2 Spectroscopic identification of the phenyltelluryl radical and its reactivity toward molecular oxygen

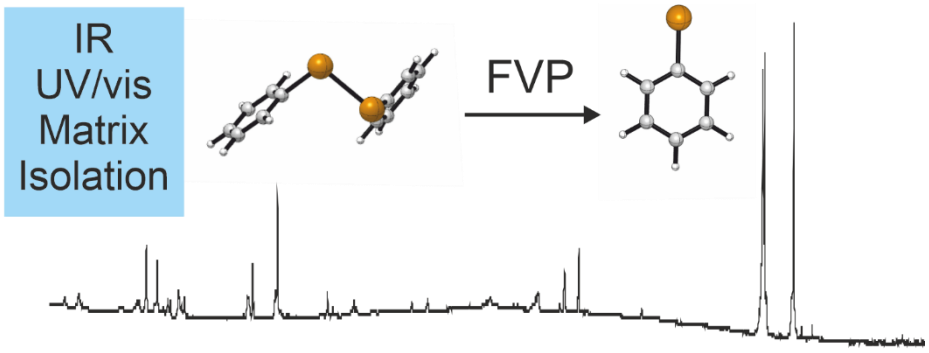

Abstract. The phenyltelluryl radical was prepared by high-vacuum flash pyrolysis of diphenyl ditelluride and was chacracterized by matrix isolation IR and UV/Vis spectroscopy. After doping the matrix with molecular oxygen and allowing bimolecular reactions, the hitherto unkown phenyltelluro peroxy radical formed and was identified *via* IR spectroscopy. Irradiation with light at λ = 436 nm leads to isomerization to the thermodynamically more stable novel phenyltelluroyl radical. All experimental findings agree well with density functional theory (UB3LYP/Def2QZVPP and UM06-2X/Def2QZVPP) computations.

Reproduced from Reference "Spectroscopic identification of the phenyltelluryl radical and its reactivity toward molecular oxygen", F. Keul, A. Mardyukov, P. R. Schreiner, *Phys. Chem. Chem. Phys.*, **2019**, 21, 25797-25801, DOI: 10.1039/C9CP05112K with permission from the Royal Society of Chemistry.

PCCP

PAPER

View Article Online
View Journal | View Issue

Published on 08 November 2019. Downloaded by UNIVERSITAT GIESSEN on 4/16/2020 1:33:46 PM.

Check for updates

Cite this: *Phys. Chem. Chem. Phys.*, 2019, **21**, 25797

Spectroscopic identification of the phenyltelluryl radical and its reactivity toward molecular oxygen†

Felix Keul, Artur Mardyukov * and Peter R. Schreiner

Received 16th September 2019,
Accepted 7th November 2019

DOI: 10.1039/c9cp05112k

rsc.li/pccp

The phenyltelluryl radical was prepared by high-vacuum flash pyrolysis of diphenyl ditelluride and was chacracterized by matrix isolation IR and UV/Vis spectroscopy. After doping the matrix with molecular oxygen and allowing bimolecular reactions, the hitherto unkown phenyltelluro peroxy radical formed and was identified *via* IR spectroscopy. Irradiation with light at λ = 436 nm leads to isomerization to the thermodynamically more stable novel phenyltelluroyl radical. All experimental findings agree well with density functional theory (UB3LYP/Def2QZVPP and UM06-2X/Def2QZVPP) computations.

Introduction

Organotellurium compounds show great potential as antioxidant and anti-cancer drugs[1–4] and are used as reagents in living radical polymerisations[5–8] as well as other reactions including stereospecific cross-coupling.[9–12] The postulated active species in these transformations, the telluryl radicals, have not yet been characterized spectroscopically. Organotelluryl radicals are versatile in living radical polymerizations due to molecular weight control, functional group tolerance, terminal polymer transformations, and ease of generation of the initiating system.[5,13,14] Another field of application is carbotelluration and aryltelluro group transfer, with primary, secondary, tertiary alkyl, and benzyl tellurides being suitable substrates.[15,16] Many reaction types are possible, for example, the synthesis of silylated allyl alcohols by domino/sequential radical-coupling reactions with the phenyltelluryl radical.[17] Furthermore, three-component coupling reactions between silyltellurides, carbonyl compounds and isonitriles were reported.[18] Based on the reactions between phenyltelluryl radicals and isonitriles an intramolecular cyclization reaction leads to quinolones (Scheme 1).[19]

A common method to generate the telluryl radical is photolysis and/or heating of diorganyl tellurides and diphenyl ditelluride in the presence of azobisisobutyronitrile (AIBN), which initiates a free radical chain reaction.[15,20] The rotational constant, spin–orbit constant, and molecular *g*-factor of the hydrotelluryl radical (HTe•), the smallest well-characterized Te-centered radical, were determined through paramagnetic resonance spectroscopy (EPR).[21]

The first step in the hydrotelluration of alkynes is the formation of an organic tellurium-centered radical by homolytic bond cleavage of the tellurium hydrogen bond of tellurol. After addition of the alkyne the propagation begins. The vinylic radical abstracts a hydrogen of tellurol and forms the final product and a telluryl radical.[22] Bell *et al.* showed that the formation of phenyltelluryl radicals from diphenyl ditelluride is a two-step procedure.[23] In the first step, dialkyl ditelluride disproportionates to dialkyl telluride under disposal of tellurium. In the second step, dialkyl telluride dissociates homolytically to form an alkyl telluryl and an alkyl radical.[23]

The reactivity of telluryl radicals is well known, but, to the best of our knowledge, these radicals have not yet been isolated and spectroscopically characterized. The preparation and isolation of the phenyltelluryl radical **1** contributes to a better understanding of the properties and the reactivity of this important class of reactive intermediates. Here we report the generation of the elusive radical **1** under matrix isolation conditions and its spectroscopic characterization by infrared (IR) and UV/Vis spectroscopy. Recently, we reported the generation and isolation of the phenylthiyl, phenylselenyl, and thiuram radicals by high-vacuum flash pyrolysis (HVFP) *via* cleavage of S–S bond and Se–Se bond, respectivly.[24–26] In the

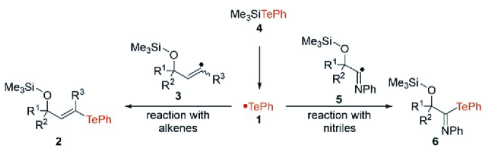

Scheme 1 A selection of synthetic applications of reactions with organotellurium compounds.

Institute of Organic Chemistry, Justus Liebig University, Heinrich-Buff-Ring 17, 35392 Giessen, Germany. E-mail: artur.mardyukov@org.chemie.uni-giessen.de

† Electronic supplementary information (ESI) available. See DOI: 10.1039/c9cp05112k

Published on 08 November 2019. Downloaded by UNIVERSITAT GIESSEN on 4/16/2020 1:33:46 PM.

present work we present an analogous procedure for the generation and isolation of **1** from diphenyl ditelluride **7**. Furthermore, we report its primary reaction with molecular oxygen.

Results and discussion

The phenyltelluryl radical was prepared by HVFP of **7** at 650 °C and subsequently trapped and isolated in an inert argon matrix at 10 K. In the thermolytic reaction a radical pair is produced by the homolytic bond cleavage of the Te–Te bond in **7** (Scheme 2). The matrix IR spectrum shows strong IR bands at 730 and 686 cm^{-1} (Fig. 1a). These bands are assigned to the C–H out of plane vibrational modes of the phenyl ring. Based on UB3LYP/Def2QZVPP computations, the bands at 1577, 1434, 1056, and 997 cm^{-1} of medium intensity were also attributed to **1** (Fig. 1). There is good agreement between experimental and computed spectra (Table 1, for details see Table S1, ESI†).

Time dependent DFT computations at TD-UB3LYP/Def2QZVPP show two strong electronic transitions at 311 nm (f = 0.0467) and 440 nm (f = 0.0599) and four weaker transitions at 287 nm (f = 0.0012), 299 nm (f = 0.0006), 384 nm (f = 0.0023), and 491 nm (f = 0.001). The measured UV/Vis spectrum of the matrix isolated pyrolysate shows strong absorptions (Fig. 2). The long wavelength absorptions in the 440 nm range display a pronounced vibrational fine structure. According to the orbitals involved in the electronic excitations, the absorption band in the visible region is an n–π* transition, while the strong band at 311 nm corresponds to a π–π* transition (Fig. S1, ESI†).

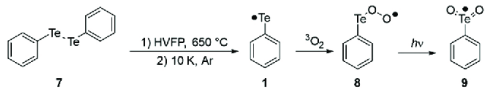

Scheme 2 The phenyltelluryl radical **1** generated by high-vacuum flash pyrolysis (HVFP) of diphenyl ditelluride **7** and subsequent trapping and isolation in an inert argon matrix 10 K. Warming in a matrix doped with molecular oxygen leads to the phenyltelluride peroxy radical **8** that photochemically isomerizes to the phenyltelluroyl radical **9**.

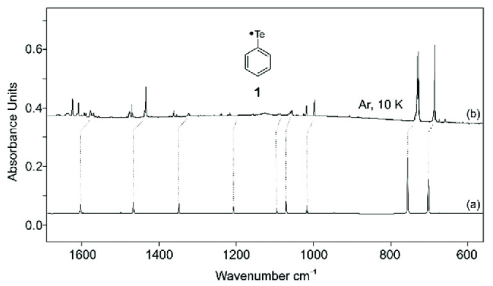

Fig. 1 (a) Harmonic IR spectrum of **1** computed at UB3LYP/Def2QZVPP (unscaled); (b) IR spectrum of matrix isolated products after pyrolysis of **7** in Ar at 10 K; the pyrolysis temperature was 650 °C.

Table 1 Experimental (Ar matrix, 10 K) and computed IR frequencies of **1**, band origins in cm^{-1}, computed intensities (km mol^{-1}) in parentheses

Mode	Computed[a]	Ar, 10 K[b]	Sym	Assignment (approx.)
25	1603 (7.8)	1577 (m)	a_1	C=C str
23	1499 (1.2)	1483 (w)	a_1	C–H def
22	1466 (11.6)	1434 (s)	b_2	C–H def
21	1349 (6.8)	1323 (m)	b_2	C–H def
19	1207 (3.7)	1183 (w)	a_1	C–H def
17	1095 (2.8)	1085 (w)	b_2	Ring distortion
16	1070 (9.3)	1056 (m)	a_1	C–Te str. + ring dist.
13	1016 (4.4)	997 (m)	a_1	Ring distortion
9	756 (39.5)	730 (s)	b_1	C–H o.o.p. def
8	703 (31.3)	686 (s)	b_1	C–H o.o.p. def
7	675 (0.4)	659 (w)	a_1	C–Te str. + ring dist.
5	453 (4.2)	440 (m)	b_1	Ring breathing

[a] UB3LYP/Def2QZVPP, anharmonic approximation, unscaled frequencies, intensities (in parentheses) in km mol^{-1}. [b] Experiment: argon matrix, 10 K; approximate relative intensities (w: weak, m: medium, s: strong).

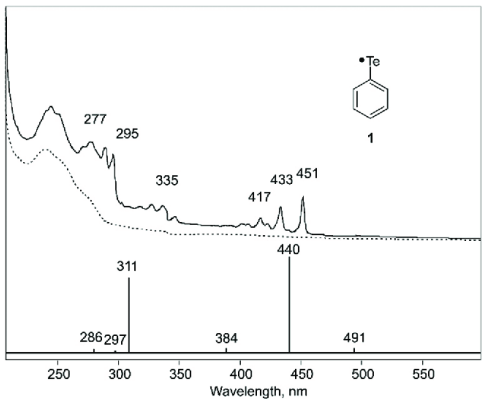

Fig. 2 Experimental UV/Vis spectrum of the matrix isolated pyrolysate (black) and background spectra (dashed, grey); computed spectrum of **1** at the TD-UB3LYP/Def2QZVPP level of theory (bottom).

Computational details

The phenyltelluryl radical **1** is C_{2v} symmetric with a $^2B_1$ electronic ground state at the UB3LYP/Def2QZVPP level of theory. We computed the geometric parameters of the known sulphur- and selenium analogues at the same level of theory for comparison with **1**.[24,25] Of course, C–Te bond (2.102 Å) is longer than a typical C–Se (1.915 Å) or C–S bond (1.756 Å), while the C–C bonds of the phenyl rings of **1**, the phenylselenyl radical (PhSe•, **10**) and the phenylthionyl radical (PhS•, **11**) show only negligible bond length differences. The homolytic Te–Te bond dissociation energy (BDE) of **7** is 38.8 kcal mol^{-1} (including zero point vibrational energy correction (ZPVE), denoted as ΔH_0). Diphenyl selenide (52.0 kcal mol^{-1}) and diphenyl disulphide (57.9 kcal mol^{-1}) show higher BDEs resulting from more loosely bound electrons in the tellurium 4p-orbital as compared to Se and S.

This journal is © the Owner Societies 2019

Published on 08 November 2019. Downloaded by UNIVERSITAT GIESSEN on 4/16/2020 1:33:46 PM.

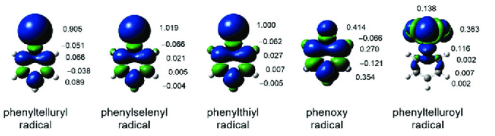

Fig. 3 Computed spin densities of **1**, the phenylselenyl, phenylthiyl, phenoxy, and phenyltelluroyl radicals at UB3LYP/Def2QZVPP. The chalcogen atom is at the top in all cases.

We also computed the spin densities of the radicals at the same level of theory to determine where most of the spin localizes. The tellurium atom of **1** shows a high spin density of 0.905 (Fig. 3), similar to the phenylselenyl and phenylthiyl radicals but in stark contrast to other highly delocalized aryl radicals like such as the phenoxy radical that shows significant delocalization over the entire phenyl ring.[24,25,28] This can be explained by the larger atomic orbital (AO) size of the higher chalcogenides that reduces the overlap with the carbon-centered p-orbitals of the phenyl ring of **1** (Fig. 3).

We compared the thermodynamic stabilities of the phenyl chalcogenyl radicals using homodesmotic Scheme 3 with the benzylic radical and toluene as reference points. The ΔH_r values suggest that **1** is by far the thermodynamically most stable radical:[25] ΔH_r = 21.2 kcal mol^{-1} X = Te, 8.4 kcal mol^{-1} X = Se, 0.4 kcal mol^{-1} X = S, and 2.6 kcal mol^{-1} X = O in this series, relative to the benzyl radical. Hence, it comes as no surprise that **1** is particularly suitable as a well-controllable initiator in living radical polymerization reactions. These values also underscore why it is particularly selective in stereospecific radical reactions.

Phenyltelluryl peroxy radical 8

The preparation and matrix isolation of **1** also allowed us to probe its reaction with molecular oxygen to the hitherto unknown phenyltelluryl peroxy radical **8**. This reaction is key to understanding the antioxidant properties of **1**. Radical **1** was prepared in the same way as before, but the matrix was doped with molecular oxygen (0.1–2.0%); warming of the matrix to 30 K allows bimolecular reactions. The IR spectra recorded after re-cooling the matrix to 10 K show good agreement between the experimental and computed spectra. The most intense band at 1125 cm^{-1} fits well with C–H in-plane vibrational modes of the phenyl ring. The medium intense bands 1437 cm^{-1}, 735 cm^{-1}, and 686 cm^{-1} are also attributed to **8** (Fig. 4 and Tables S2–S3, ESI†). Based on the computations **8** displays *cis* (**8c**, C_s) and *trans* (**8t**, C_s) conformers, which are nearly isoenergetic and display ^{2}A electronic ground states. The rotamerization barrier amounts to only 0.9 kcal mol^{-1}. The addition of molecular oxygen ($^3O_2$) is barrierless and mildly exothermic (−1.3 kcal mol^{-1}, Fig. 5). As the computed IR spectra of **8c** and **8t** are very similar they cannot be distinguished. The spin density is mostly distributed between two oxygens with the terminal oxygen having the higher spin density.

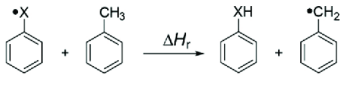

Scheme 3 Homodesmotic reaction between chalcogen radicals and toluene to assess relative radical stability.

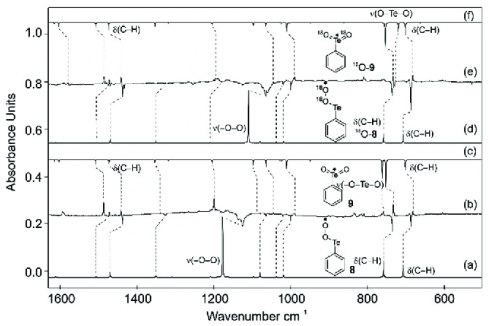

Fig. 4 (a) Computed harmonic IR spectrum of **8**; (b) IR difference spectra after photoirradiation with a wavelength of λ = 436 nm after 15 min irradiation time in Ar at 10 K. Downward bands of **8** disappear, while upward bands assigned to **9** appear; (c) computed IR spectrum of **9**; (d) computed IR spectrum of ^{18}O-**8**; (e) IR difference spectra after photoirradiation with a wavelength of λ = 436 nm after 15 min irradiation time in Ar at 10 K. Downward bands assigned to ^{18}O-**8** disappear, upward bands are assigned to ^{18}O-**9**; (f) computed IR spectrum of ^{18}O-**9**. All computations were done at the UB3LYP/Def2QZVPP level of theory and the spectra were not scaled.

Photochemistry of 8

Irradiation of a matrix containing **8** at λ = 436 nm results in the disappearance of all IR bands attributed to **8** and new bands at 1487 cm^{-1}, 1441 cm^{-1}, 1200 cm^{-1}, 758 cm^{-1}, and 731 cm^{-1} appear (Fig. 4, for details see Table S4). These IR bands were assigned to the C–H stretching and out-of-plane vibrational modes of the phenyl ring of isomer **9**. The optimized C_s symmetric structure has an ^{2}A′ electronic ground state, with the electron spin

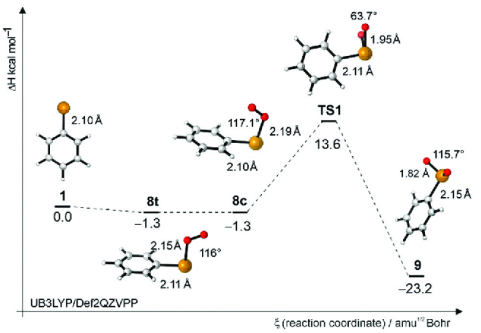

Fig. 5 Potential energy hypersurface of the reaction of the phenyltelluryl radical **1** with molecular oxygen. Computed at the UB3LYP/Def2QZVPP level of theory.

Published on 08 November 2019. Downloaded by UNIVERSITAT GIESSEN on 4/16/2020 1:33:46 PM.

density being delocalized in the O–Te–O moiety (Fig. 3). The rearrangement of **8c** to **9** *via* transition state **TS1** is associated with a barrier of 14.9 kcal mol^{-1}. The overall reaction from **8** to **9** is −21.9 kcal mol^{-1} exothermic (Fig. 5).

To validate our results, we also performed experiments with $^{18}O_2$. In the case of **8** there is a strong ^{18}O isotopic shift of −60 cm^{-1} (computed: −60 cm^{-1}) for the O–O stretching vibrational mode located at 1125 cm^{-1}. Due to ^{18}O isotopic substitution the O–Te–O symmetric vibration is shifted by 33 cm^{-1} (computed: −41 cm^{-1}) to 758 cm^{-1} (Table S4, ESI†).

Experimental details

Matrix apparatus design

For the matrix isolation studies, we used an APD Cryogenics HC-2 cryostat with a closed-cycle refrigerator system, equipped with an inner CsI window for IR measurements. Spectra were recorded with a Bruker IFS 55 FT-IR spectrometer with a spectral range of 4500–400 cm^{-1} and a resolution of 0.7 cm^{-1} and UV/Vis spectra were recorded with a JASCO V-670 spectrophotometer. For the combination of high-vacuum flash pyrolysis with matrix isolation, we employed a small, home-built, water-cooled oven, which was directly connected to the vacuum shroud of the cryostat. The pyrolysis zone consisted of an empty quartz tube with an inner diameter of 8 mm, which was resistively heated over a length of 50 mm by a coaxial wire. The temperature was monitored with a NiCr–Ni thermocouple. Diphenyl ditelluride **7** (Sigma-Aldrich) was evaporated (**7**:60 °C) from a storage bulb into the quartz pyrolysis tube. At a distance of approximately 50 mm, all pyrolysis products were co-condensed with a large excess of argon (typically 60–120 mbar from a 2000 mL storage bulb) on the surface of the matrix window at 10 K (20 K). Several experiments with pyrolysis temperatures ranging from 650 °C were performed in order to determine the optimal pyrolysis conditions. A high-pressure mercury lamp (HBO 200, Osram) with a monochromator (Bausch & Lomb) was used for irradiation.

Computations

All geometries were optimized and characterized as minima by means of analytic harmonic vibrational frequency computations at the UB3LYP/Def2QZVPP and UM06-2X/Def2QZVPP[29,30] levels of theory. The grid size was defined with 99 radial shells and 590 angular points and convergence criteria was set with the keyword "tight". All computations were performed with the Gaussian16 program package.[31]

Conclusions

We generated and spectroscopically characterized the phenyltelluryl radical by matrix isolation IR and UV/Vis spectroscopy. All findings are supported by DFT computations. We examined the hitherto unreported reactivity of the phenyltelluryl radical with molecular triplet oxygen. During the reaction the novel phenyltelluro peroxy radical formed. The IR spectra match the computed spectra very well. Photoirradiation at λ = 436 nm leads to the thermodynamically more stable phenyltelluroyl radical, which is also a new species.

The stability of phenyltelluryl radical is readily reflected in the relatively low Te–Te bond dissociation enthalpy of 38.8 kcal mol^{-1}, and the localization of the spin density on the tellurium atom. Energy comparisons with a homodesmotic equation also demonstrate the relatively high stability of **1** as compared to the other phenyl chalcogenyl radicals. Radical **1** is of comparable stability as the benzyl radical. Knowledge of the properties of these radicals provides valuable insights into the mechanisms of their formation and oxidation reactions, and we hope that our results are also relevant to understand radical reactions with such chalcogenyl radicals in, for instance, polymerization processes.[27]

Conflicts of interest

There are no conflicts to declare.

Acknowledgements

This research was supported by the Justus Liebig University.

Notes and references

1 E. Wieslander, L. Engman, E. Svensjö, M. Erlansson, U. Johansson, M. Linden, C.-M. Andersson and R. Brattsand, *Biochem. Pharmacol.*, 1998, **55**, 573–584.
2 J. Kanski, J. Drake, M. Aksenova, L. Engman and D. A. Butterfield, *Brain Res.*, 2001, **911**, 12–21.
3 D. S. Ávila, P. Gubert, A. Palma, D. Colle, D. Alves, C. W. Nogueira, J. B. T. Rocha and F. A. A. Soares, *Brain Res. Bull.*, 2008, **76**, 114–123.
4 L. Engman, N. Al-Maharik, M. McNaughton, A. Birmingham and G. Powis, *Bioorg. Med. Chem.*, 2003, **11**, 5091–5100.
5 S. Yamago, K. Iida and J.-I. Yoshida, *J. Am. Chem. Soc.*, 2002, **124**, 13666.
6 Y. Kwak, A. Goto, T. Fukuda, Y. Kobayashi and S. Yamago, *Macromolecules*, 2006, **39**, 4671–4679.
7 S. Yamago, Y. Ukai, A. Matsumoto and Y. Nakamura, *J. Am. Chem. Soc.*, 2009, **131**, 2100–2101.
8 Y. Nakamura, T. Arima, S. Tomita and S. Yamago, *J. Am. Chem. Soc.*, 2012, **134**, 5536–5539.
9 M. J. Dabdoub, V. B. Dabdoub and J. P. Marino, *Tetrahedron Lett.*, 2000, **41**, 437–440.
10 R. E. Barrientos-Astigarraga, P. Castelani, J. V. Comasseto, H. B. Formiga, N. C. da Silva, C. Y. Sumida and M. C. L. Vieira, *J. Organomet. Chem.*, 2001, **623**, 43–47.
11 S. Yamago, H. Miyazoe, R. Goto, M. Hashidume, T. Sawazaki and J.-I. Yoshida, *J. Am. Chem. Soc.*, 2001, **123**, 3697–3705.
12 A. L. Braga, D. S. Lüdtke, F. C. Vargas, R. K. Donato, C. C. Silveira, H. A. Stefani and G. Zeni, *Tetrahedron Lett.*, 2003, **44**, 1779–1781.
13 S. Yamago, K. Iida and J.-I. Yoshida, *J. Am. Chem. Soc.*, 2002, **124**, 2874–2875.

 This journal is © the Owner Societies 2019

Published on 08 November 2019. Downloaded by UNIVERSITAT GIESSEN on 4/16/2020 1:33:46 PM.

14 S. Yamago, K. Iida, M. Nakajima and J.-I. Yoshida, *Macromolecules*, 2003, **36**, 3793–3796.
15 L. B. Han, K. Ishihara, N. Kambe, A. Ogawa, I. Ryu and N. Sonoda, *J. Am. Chem. Soc.*, 1992, **114**, 7591–7592.
16 L.-B. Han, K.-I. Ishihara, N. Kambe, A. Ogawa and N. Sonoda, *Phosphorus Sulfur Relat. Elem.*, 1992, **67**, 243–246.
17 S. Yamago, M. Miyoshi, H. Miyazoe and J. Yoshida, *Angew. Chem., Int. Ed.*, 2002, **41**, 1407–1409.
18 H. Miyazoe, S. Yamago and J. I. Yoshida, *Angew. Chem.*, 2000, **112**, 3815–3817.
19 T. Mitamura, K. Iwata and A. Ogawa, *Org. Lett.*, 2009, **11**, 3422–3424.
20 A. E. D. McQueen, P. N. Culshaw, J. C. Walton, D. Shenai-Khatkhate, D. J. Cole-Hamilton and J. B. Mullin, *J. Cryst. Growth*, 1991, **107**, 325–330.
21 H. Radford, *J. Chem. Phys.*, 1964, **40**, 2732–2733.
22 A. F. Keppler, G. Cerchiaro, O. Augusto, S. Miyamoto, F. Prado, P. Di Mascio and J. V. Comasseto, *Organometallics*, 2006, **25**, 5059–5066.
23 W. Bell, D. J. Cole-Hamilton, P. N. Culshaw, A. E. D. McQueen, D. Shenai-Khatkhate, J. C. Walton and J. E. Hails, *J. Organomet. Chem.*, 1992, **430**, 43–52.
24 A. Mardyukov and P. R. Schreiner, *Phys. Chem. Chem. Phys.*, 2016, **18**, 26161–26165.
25 A. Mardyukov, Y. A. Tsegaw, W. Sander and P. R. Schreiner, *Phys. Chem. Chem. Phys.*, 2017, **19**, 27384–27388.
26 A. Mardyukov, F. Keul and P. R. Schreiner, *J. Phys. Chem. A*, 2019, **13**, 4937–4941.
27 V. Bhanu and K. Kishore, *Chem. Rev.*, 1991, **91**, 99–117.
28 R. Crespo-Otero, K. Bravo-Rodriguez, S. Roy, T. Benighaus, W. Thiel, W. Sander and E. Sánchez-García, *Chem. Phys. Chem.*, 2013, **14**, 805–811.
29 F. Weigend, *Phys. Chem. Chem. Phys.*, 2006, **8**, 1057–1065.
30 F. Weigend and R. Ahlrichs, *Phys. Chem. Chem. Phys.*, 2005, **7**, 3297–3305.
31 M. J. Frisch, G. W. Trucks, H. B. Schlegel, G. E. Scuseria, M. A. Robb, J. R. Cheeseman, G. Scalmani, V. Barone, G. A. Petersson, H. Nakatsuji, X. Li, M. Caricato, A. V. Marenich, J. Bloino, B. G. Janesko, R. Gomperts, B. Mennucci, H. P. Hratchian, J. V. Ortiz, A. F. Izmaylov, J. L. Sonnenberg, F. Ding Williams, F. Lipparini, F. Egidi, J. Goings, B. Peng, A. Petrone, T. Henderson, D. Ranasinghe, V. G. Zakrzewski, J. Gao, N. Rega, G. Zheng, W. Liang, M. Hada, M. Ehara, K. Toyota, R. Fukuda, J. Hasegawa, M. Ishida, T. Nakajima, Y. Honda, O. Kitao, H. Nakai, T. Vreven, K. Throssell, J. A. Montgomery Jr., J. E. Peralta, F. Ogliaro, M. J. Bearpark, J. J. Heyd, E. N. Brothers, K. N. Kudin, V. N. Staroverov, T. A. Keith, R. Kobayashi, J. Normand, K. Raghavachari, A. P. Rendell, J. C. Burant, S. S. Iyengar, J. Tomasi, M. Cossi, J. M. Millam, M. Klene, C. Adamo, R. Cammi, J. W. Ochterski, R. L. Martin, K. Morokuma, O. Farkas, J. B. Foresman and D. J. Fox, *Gaussian16 Rev. B01*, Gaussian, Inc., Wallingford CT, 2016.

2.3 Generation and Reactivity of the Vinyltelluryl Radical

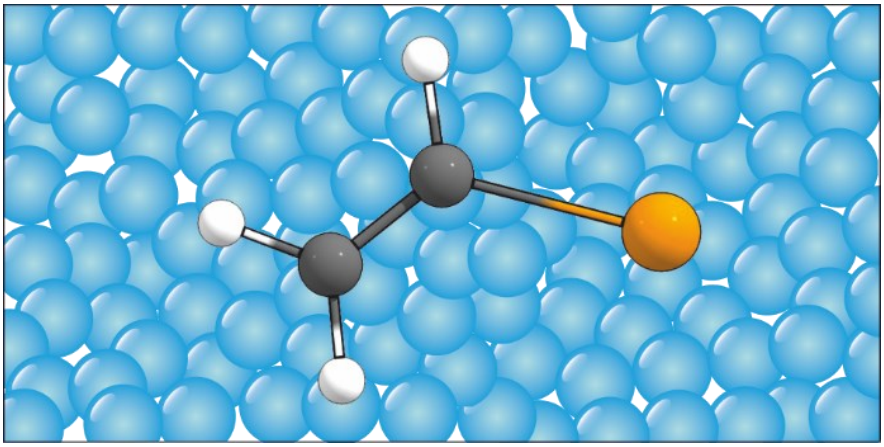

Abstract. The vinyltelluryl radical was prepared by high-vacuum flash pyrolysis from the corresponding divinylditelluride and trapped in an argon matrix at 10 K. The title compound was characterized by IR and UV/Vis spectroscopy and all experimental data match well with the density functional theory at UB3LYP/def2-QZVPP level. According to UB3LYP/def2-QZVPP computations, the electron density is mainly localized on the Te atom. The vinylogy principle for the vinyltelluryl radical is not applicable due to the lack of delocalization of spin density. Upon irradiation of the matrix vinyltelluryl radical with light λ = 365 nm rearranges to H–Te•…acetylene complex. Doping the matrix with molecular oxygen leads to the hitherto unknown vinyltelluro peroxy radical. The latter isomerizes to the thermodynamically more stable vinyltelluroyl radical by irradiation with light λ = 523 nm.

Reproduced from Reference "Generation and Reactivity of the Vinyltelluryl Radical", F. Keul, A. Mardyukov, *Phys. Chem. Chem. Phys.*, **2022**, *24*, 5129-15134, DOI: 10.1039/d2cp01658c with permission from the Royal Society of Chemistry.

Published on 30 May 2022. Downloaded by UNIVERSITAT GIESSEN on 8/21/2022 9:54:56 AM.

PCCP

ROYAL SOCIETY OF CHEMISTRY

PAPER

View Article Online
View Journal | View Issue

Check for updates

Cite this: *Phys. Chem. Chem. Phys.*, 2022, **24**, 15129

Received 10th April 2022,
Accepted 30th May 2022

DOI: 10.1039/d2cp01658c

rsc.li/pccp

Generation and reactivity of vinyltelluryl radical†

Felix Keul and Artur Mardyukov *

Vinyltelluryl radical was prepared by high-vacuum flash pyrolysis from the corresponding divinylditelluride and trapped in an argon matrix at 10 K. The title compound was characterized by IR and UV/Vis spectroscopy, and all experimental data match well with density functional theory at the UB3LYP/def2-QZVPP level. According to UB3LYP/def2-QZVPP computations, the spin density is mainly localized on the Te atom. The vinylogy principle for the vinyltelluryl radical is not applicable due to the lack of delocalization of spin density. Upon irradiation of the matrix with light (λ = 365 nm), the vinyltelluryl radical rearranges to a H–Te$^{\bullet}\cdots$acetylene complex. Doping the matrix with molecular oxygen leads to the hitherto unknown vinyltelluro peroxy radical. The latter isomerizes to the more thermodynamically stable vinyltelluroyl radical by irradiation with light at λ = 523 nm.

Introduction

Free radicals are reactive open-shell species that play an important role in chemistry[1] and biology,[2] and they are key oxidizing agents in the global atmosphere.[3] Several factors impact the stability of free radicals, among which conjugative resonance stabilization is a popular strategy in making stable radicals. The allyl radical (**1**) is a prototype example of conjugative resonance stabilization, whose delocalized unpaired electron is in conjugation with the π-system (Scheme 1(A)). Radical **1** represents the simplest odd alternating hydrocarbon with a negative spin density of the central carbon, as determined by electron paramagnetic resonance (ESR) spectroscopy.[4,5] According to computations, **1** displays a C_{2v} symmetry and C–C bond lengths between single and double bonds,[6] with the bond dissociation energy (BDE) of propene at 88.4 ± 0.4 kcal mol^{-1}.[7,8]

The vinoxy radical (**2**) is the simplest vinyl chalcogen radical (Scheme 1(A)). Radical **2** is considered a key intermediate in the gas phase reaction of olefins with oxygen[9,10] in atmospheric chemistry[11] and has therefore been extensively studied both experimentally[12] and theoretically.[13–17] Direct reactions of **2** are investigated by time-of-flight mass spectrometry (TOF-MS),[18] laser-induced fluorescence,[19] and excimer laser photolysis.[20] The heavier congener of the vinoxy radical (Scheme 1(A)), the vinylthio radical (**3**), has been the target of numerous experimental and theoretical studies due to its involvement as an important intermediate in hydrocarbon oxidation processes.[21] Theoretical studies consider a sulfur-center-based radical.[22] The first mass spectroscopic evidence was reported in 1992 by Huber *et al.*, by photodissociation of thiirane at a 193 nm molecular beam.[23] In 2007, the first spectroscopic observation of **3** was reported by laser-induced fluorescence and Fourier-transform microwave spectroscopy.[24] Moreover, very recently, the vinylsulfinyl radical CH$_2$=C(H)SO$^{\bullet}$ was isolated in cryogenic matrixes and characterized with IR and UV/Vis spectroscopy.[25]

The vinylselenyl radical (**4**) and vinyltelluryl radical (**5**) remain elusive (Scheme 1(B)), despite the fact that selenyl and telluryl radicals are highly relevant in synthesis,[26,27] biological processes,[28] as well as living radical polymerizations.[29,30] The parent H–Te$^{\bullet}$ radical was first observed by Radford *via* electron paramagnetic resonance (EPR) in 1964.[31] The ground state of the H–Te$^{\bullet}$ radical is $^2\Pi_{3/2}$, with an inverted multiplet structure.[31] The molecular constants of the H–Te$^{\bullet}$ and D–Te$^{\bullet}$ radicals, B_0 = 6.06538(12) and 3.07142(18) cm^{-1}, respectively, were determined by Fink and co-worker in 1989 using near-infrared spectroscopy and, five years later, Brown *et al.* using infrared spectroscopy (B_0 = 6.065064(37) cm^{-1} for H–Te$^{\bullet}$).[32,33] Donovan *et al.* reported the UV/Vis spectrum for Te–H$^{\bullet}$ radical and identified the Rydberg series and the first ionization potential.[34]

Recently, we reported the generation and matrix isolation of the phenyltelluryl radical and its reaction with oxygen,[35] which

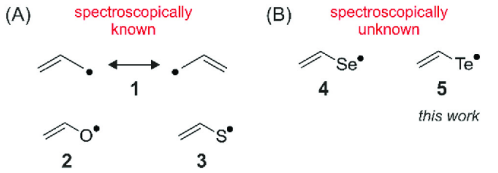

Scheme 1 Allyl radical (**1**) and vinyl chalcogenide radicals (**2–5**).

Institute of Organic Chemistry Justus-Liebig University, Heinrich-Buff-Ring 17, 35392 Giessen, Germany. E-mail: artur.mardyukov@org.chemie.uni-giessen.de

† Electronic supplementary information (ESI) available. See DOI: https://doi.org/10.1039/d2cp01658c

Published on 30 May 2022. Downloaded by UNIVERSITAT GIESSEN on 8/21/2022 9:54:56 AM.

is an important reactive intermediate in radical polymerization reactions.[36–38] As part of our ongoing studies on heteroatom radicals, we are now able to prepare and isolate in argon matrix the elusive vinyltelluryl radical. Herein, we report the first IR and UV/Vis spectroscopic characterization of **5** together with its hitherto unexplored photochemistry and reactivity with molecular oxygen.

Results and discussion

We recently reported the preparation of phenylthiyl, phenylselenyl, and phenyltelluryl radicals by thermal or photochemical decomposition of the corresponding diphenyl dichalcogenides.[35,39,40] In line with previous studies, we first attempted the generation of **5** by photolysis of divinylditelluride (**6**) and subsequent trapping and isolation in an inert argon matrix at 10 K (Scheme 2). Photolysis of the matrix-isolated **6** produces a large amount of acetylene, evident by the strong absorption bands at 3265 and 738 cm^{-1} (Fig. S1, ESI†) due to the C–H stretching and C–H deformation modes. The bands at 3265 and 738 cm^{-1} are shifted from the unperturbed C–H stretching and C–H deformation modes of acetylene[41] at 3288 and 737 cm^{-1} by −23 and +1 cm^{-1}, which are assigned to the H–Te$^{\bullet}\cdots$H–C≡C–H complex (**8**) (*vide infra*). In addition, we found a weak band at 2025 cm^{-1}, which is attributed to H–Te stretching mode in **8**. These bands correlate well with the computed bands for structure **8**. Despite our extensive efforts to prepare **5** through the photochemical route in noble gas matrices were unsuccessful. Therefore, we turned our attention to the thermal generation of **5**. Pyrolysis of **6** at 800 °C and subsequent trapping of pyrolysis products at 10 K show new IR bands that were not present in the photochemical route. The infrared spectrum of the flash vacuum pyrolysis (FVP) products of **6** shows several new absorptions, next to some unreacted starting material and the usual impurities (*e.g.* H_2O, CO_2) often found in FVP experiments. In addition, we observed new unreported signals that we assigned to **5**; note that no IR bands are present for **8**. For example, the strong IR band at 965 and 923 cm^{-1} are attributed to the C–H and CH_2 out-of-plane bending modes of **5** (Table S1, ESI†). With the help of computations, other weak and moderate-intensity IR bands at 3036, 2995, 2988, 1553, 1368, 1245, and 480 cm^{-1} were assigned to **5**. Altogether, the good agreement between the experimental and computed (UB3LYP/def2-QZVPP) IR frequencies of **5** underlines the successful preparation of **5** (Fig. 1, Fig. S2 and Table S1, ESI†).

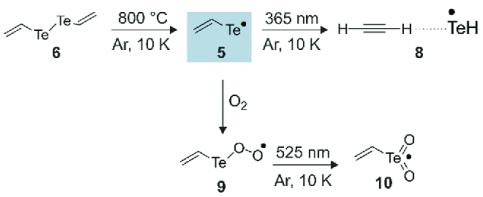

Scheme 2 Vinyltelluryl radical **5** generated through pyrolysis of divinylditelluride **6** trapping in an argon matrix and subsequent (photo)reactivity.

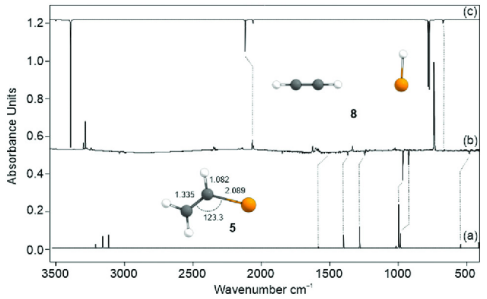

Fig. 1 IR spectra showing the pyrolysis products of **6** upon subsequent trapping in an argon matrix at 10 K. (a) IR spectrum of **5** computed at UB3LYP/def2-QZVPP (unscaled). (b) IR difference spectra showing the photochemistry of **5** after irradiation with λ = 365 nm in argon at 10 K. Downward bands assigned to **5** disappear, while upward bands assigned to **8a** appear after 15 min irradiation time. (c) IR spectrum of **8a** computed at UB3LYP/def2-QZVPP (unscaled).

Moreover, UV irradiation (λ = 365 nm) of the matrix containing **5** results in the disappearance of all its IR bands and the simultaneous appearance of a new set of IR bands at 3283, 2065, 739, 736, 667, and 662 cm^{-1}. The band positions are identical in the photochemical experiments mentioned above and were attributed to **8** (Fig. 1). Two H–Te$^{\bullet}\cdots$H–C≡C–H complexes with stabilization energies of −0.35, −0.1 kcal mol^{-1} and −1.2, −2.6 kcal mol^{-1} (**8a** and **8b**) were localized at the UB3LYP/def2-QZVPP and UB3LYP-D3(BJ)/def2-QZVPP levels of theory, respectively (Fig. S1, ESI†). The experimentally observed IR spectrum from the photolysis of **5** nicely matched the computed spectrum of **8a** (Table S2, ESI†).

The matrix-isolated UV/Vis spectrum of **5** reveals a broad absorption transition (λ_{max} = 237 nm) and a weak absorption transition (λ_{max} = 403 nm), which is in good agreement with its computed time-dependent density functional theory (TD-DFT) spectrum. TD-B3LYP/def2-QZVPP computations for **5** evince a strong transition at 254 nm (f = 0.14; $\pi \rightarrow \pi^*$) and a weak transition at 420 nm (f = 0.0026; $n \rightarrow \pi^*$; Fig. 2 and Fig. S3, ESI†). In line with the IR experiments, upon photolysis using 365 nm light, the broad absorptions at 237 and 403 nm vanished.

According to UB3LYP/def2-QZVPP computations, radical **5** displays a planar C_s symmetry with an electronic ground state of $^2A''$. The C–Te bond distance in **5** is 2.089 Å, which is in the same range as the phenyltelluryl radical (2.102 Å).[35] The C=C bond distance is 1.336 Å, in a typical alkene range. The spin density in **5** is mainly localized on the Te atom (0.898) due to the larger atomic orbital (AO) size of tellurium; this is in marked contrast to ally radical **1**, where an unpaired electron is delocalized over a system of the conjugated π bond (Fig. S4 and S5, ESI†). The spin density in **5** is in the same range as phenylthiyl, phenylselenyl and phenyltelluryl radicals, respectively.[35,39,40]

The bond dissociation energy (BDE) of the Te–Te bond in **6** is 40.9 kcal mol^{-1} at the UB3LYP/def2-QZVPP level (including zero-point vibrational energy correction (ZPVE)). The BDEs in

This journal is © the Owner Societies 2022

Published on 30 May 2022. Downloaded by UNIVERSITAT GIESSEN on 8/21/2022 9:54:56 AM.

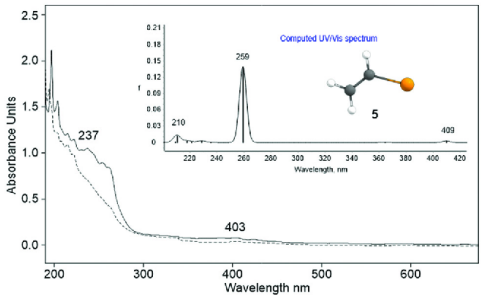

Fig. 2 Solid line: UV/Vis spectrum of **5** isolated at 10 K in Ar. Dashed line: the photochemistry of **5** after irradiation with λ = 365 nm in argon at 10 K. Inset: Computed [TD-UB3LYP/def2-QZVPP] electronic transitions for **5**.

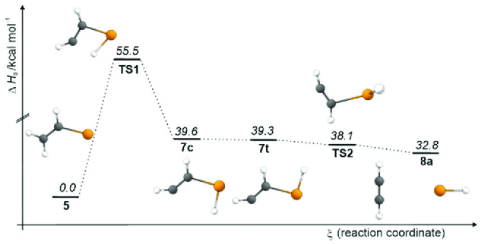

Fig. 3 Potential energy hypersurface (ΔH_0) in kcal mol^{-1} of the reaction of **5** at the UB3LYP/def2-QZVPP level of theory.

divinylselenide and divinylsufide are 41.1 and 41.9 kcal mol^{-1}, respectively. In the case of oxygen, the BDE is −16.0 kcal mol^{-1}; thus the radical is preferred because of the unfavored O–O bond (Table S3, ESI†).[42] We also computed the BDEs of the homolytic cleavage of X–H bonds (X = CH_2, O, S, Se, Te) of the heteroatom-containing vinyl alcohols; for details, see the Supporting Information (Table S3, ESI†).

Furthermore, we compared the thermodynamic stabilities of vinyl chalcogenyl radicals with the allyl radical as a reference point, using a homodesmotic reaction depicted in equation 1. The ΔH_r values suggest that **5**, with 17.3 kcal mol^{-1}, is the most thermodynamically stable radical in the row; for X = Se, ΔH_r = 11.0 kcal mol^{-1}; and X = S and O are 5.6 and 2.2 kcal mol^{-1}.

(1)

X = O, S, Se, Te

Next, we undertook detailed computational studies to elucidate the mechanism of the formation of **8** from **6**. Radical **5** is formed as a result of homolytic cleavage of the Te–Te bond in **6**. The formation of **8** from **5** is a multistep reaction. The first reaction path implies the intramolecular [1,3]H-shift from the terminal methylene group to the Te atom in **5** to give radical **7c**, with an activation barrier of 52.3 kcal mol^{-1} (**TS1**). Aside from this, we did not observe characteristic IR bands for **7** after FVP experiments indicated that the energy is insufficient in the pyrolysis zone for **5** to undergo [1,3]H-shift. The radical **7c** is a planar C_s structure with a ^{2}A′ electronic ground state. The C–Te bond distance in **7c** is slightly longer (2.146 Å) than in **5** (2.104 Å), and the C=C double bond distance of 1.288 Å is shorter than the C=C bond distance of 1.326 Å in **5**. The spin density in **7c** is mostly localized at the terminal carbon atom (0.9) (Fig. S4, ESI†). With a typical rotational barrier of 0.98 kcal mol^{-1}, **7c** interconverts to vinyl radical **7t**. The subsequent C–Te bond fission to **8** is accompanied by a low-lying barrier of −1.2 kcal mol^{-1} (**TS2**) (Fig. 3).

We also performed a natural resonance theory (NRT) analysis[43,44] at UB3LYP/def2-QZVPP, UM06-2X/def2-QZVPP, and UHF/def2-QZVPP levels of theory. In the case of X = Te, we obtained six different mesomeric structures (Scheme 3). **11a** is present in 76.9% (UM06-2X: 79.4%; UHF: 80.0%), and the corresponding **12a** in 10.4% (UM06-2X: 8.2%; UHF: 8.8%). There are four other mesomeric structures in the range of 2.7% to 3.8% (see details in ESI†). Due to the large AO of the Te atom, the unpaired electron is almost localized at the tellurium atom. For X = Se, **11b** is present in 72.5% (UM06-2X: 75.7%; UHF: 75.9%), and **12b** in 16.2% (UM06-2X: 13.4%; UHF: 14.3%). For sulfur, the ratio is 66.6% for **11c** and 23.3% for **12c** at UB3LYP/def2-QZVPP (UM06-2X: 68.7%-**11c**, 21.3%-**12c**; UHF: 70.4%-**11c**, 20.8%-**12c**). This trend also correlates with a decrease in AO size in Te > Se > S. In the case of X = O (**11d**), the ratio is 43.5% (UM06-2X: 48.7%; UHF: 48.3%) and (**12d**) 39.1% (UM06-2X: 34.5%; UHF: 41.9%). For X = CH_2, the computations predict the ratio of both to be 1 : 1 (Scheme 3).

Recently, we showed that the thermal reaction of phenyltelluryl radical with $^3O_2$ in argon matrices produces phenyltelluryl peroxy radical.[35] Analogous to the phenytelluryl radical, **5** should react with $^3O_2$ to give corresponding peroxy radicals. According to UB3LYP/def2-QZVPP computations, vinyltelluryl peroxy radical **9** displays two conformers, *cis* (**9c**) and *trans* (**9t**) forms, which are nearly isoenergetic (ΔH = 0.2 kcal mol^{-1}) and with a rotamerization barrier of only 0.5 kcal mol^{-1}. Doping argon matrices with different concentrations of oxygen (0.2–2%) resulted in significant changes in the IR spectra. For instance, strong bands at 1165 and 1115 cm^{-1} are assigned to the O–O stretching modes in **9c** and **9t**, respectively (Fig. 4 and Table S4, ESI†). With the aid of computations, the medium-intensity bands at 1236 and 960 cm^{-1} are attributed to the CH_2 in-plane and out-of-plane bending modes. To confirm our results, we also performed isotope labeling experiments using $^{18}O_2$. For example, the strong IR bands at 1165 and 1115 cm^{-1} show strong isotope redshifts of 65 and 62 cm^{-1}, in good agreement with the computed values of 70 and 68 cm^{-1},

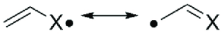

11 **12**

X = Te (a), Se (b), S (c), O (d), CH_2 (e)

Scheme 3 Mesomeric structures of **1–5**.

Published on 30 May 2022. Downloaded by UNIVERSITAT GIESSEN on 8/21/2022 9:54:56 AM.

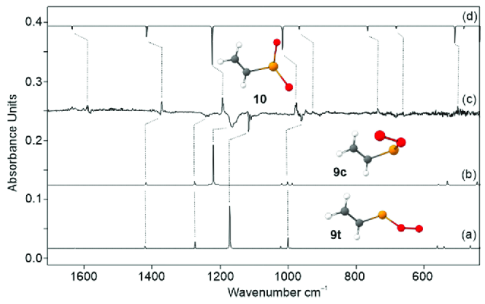

Fig. 4 (a) IR spectrum of **9t** computed at UB3LYP/def2-QZVPP (unscaled). (b) IR spectrum of **9c** computed at UB3LYP/def2-QZVPP (unscaled). (c) IR difference spectra showing the photochemistry of **9c** and **9t** after irradiation at λ = 523 nm in argon at 10 K. Downward bands assigned to **9c** and **9t** disappear, while upward bands assigned to **10** appear after 5 min of irradiation time. (d) IR spectrum of **10** computed at UB3LYP/def2-QZVPP (unscaled).

respectively. Overall, the experimentally observed IR bands match well with the computed fundamentals for **9** and $^{18}O_2$-**9** at UB3LYP/def2-QZVPP level (Table S4 and Fig. 5, Fig. S6, S7, ESI†).

The formation of **9** is also confirmed by UV/Vis spectroscopy. UV/Vis of **9** shows a strong transition at 345 nm. The band at 345 nm correlates well with the computed values for the electronic excitations of **9**. TD-UB3LYP/def2-QZVPP computations predict a strong transition at 299 nm (f = 0.167), and weak transitions at 548 (f = 0.003) and 695 nm (f = 0.002) for **9c**; 324 (f = 0.181), 519 (f = 0.05), 547 (f = 0.002) and 614 nm (f = 0.001) for **9t**. Unfortunately, due to the low extinction coefficients, the UV/Vis transitions of **9** in the range between 400 and 800 nm could not be detected (Fig. S8 and S9, ESI†).

Irradiation of the matrices containing **9** with light at λ = 523 nm results in a rapid decrease of all IR bands attributed to **9** and, simultaneously, the formation of a new set of IR bands. The IR spectrum of the new product is assigned to vinyltelluroyl radical (**10**). The most intense band at 1191 cm^{-1} is attributed to CH bending mode. In $^{18}O_2$ experiments, we found a moderate ^{18}O isotope shift for a band at 737 cm^{-1} (−16 cm^{-1} expr., −41 cm^{-1} calc.), which was assigned to the OTeO symmetric vibration of **10** (Table S5, ESI†). The transformation of **9** to **10** is associated with the barrier of 15.3 kcal mol^{-1} (**TS3**), which is an exothermic process by 21.1 kcal mol^{-1} from **9** (Fig. 5). In **9**, the spin density is mainly localized on the terminal oxygen atom (0.655 for **9c**, 0.648 for **9t**), while the oxygen atom next to the tellurium atom has a spin density of 0.422 for **9c** (0.379, **9t**); whereas in **10**, the spin density is delocalized on the OTeO moiety (Te = 0.13, O = 0.419, and 0.319)[35] (Fig. S10, ESI†).

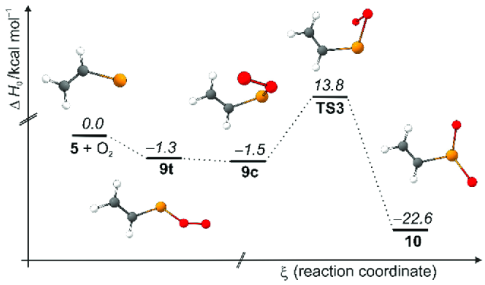

Fig. 5 Potential hypersurface of the reaction of **5** with molecular triplet oxygen ($^3O_2$) at UB3LYP/def2-QZVPP level of theory.

Conclusions

We generated and isolated the vinyltelluryl-radical **5** in an argon matrix at 10 K. The radical was spectroscopically characterized by IR and UV/Vis spectroscopy, and all findings match well with data computed at the UB3LYP/def2-QZVPP level. The stability of **5** is reflected by the low dissociation enthalpy of the Te–Te bond in divinylditelluride of 47.2 kcal mol^{-1}. According to NRT analysis, the spin density is mainly localized at the Te atom; thus, the vinylogy principle is not applicable. The high stability of the vinyltelluryl radical is also supported by hypothetical isodesmic reactions with comparative chalcogen radicals. Doping the matrix of **5** with molecular oxygen leads to the formation of a hitherto unknown vinyltelluryl peroxy radical. The latter undergoes photoisomerization into a more stable, novel vinyltelluroyl radical upon 523 nm irradiation.

Experimental

Synthesis

Compound **6** was prepared following a literature protocol.[38] Briefly, 5 mL (5.00 mmol, 1.00 equiv., 1 M in THF) vinylmagnesiumbromide and 0.635 g (5.00 mmol, 1.00 equiv.) elemental tellurium were dissolved in 27.5 mL dry THF under N_2 atmosphere and refluxed for 30 min. Then, the flask was opened, and the mixture was stirred for 1 hour at room temperature. The solvent was removed *via* distillation, and the residue was purified *via* column chromatography (hexane). Product **6** was obtained (414 mg, 27%). ^{1}H-NMR (400 MHz, $CDCl_3$): δ/ppm = 7.12 (2H, dd, J = 7.6 Hz, 9.8 Hz), 6.20 (2H, d, J = 9.8 Hz), 5.91 (2H, d, J = 16.6 Hz); ^{13}C-NMR (101 MHz, $CDCl_3$): δ/ppm = 131.3, 101.7.

Matrix apparatus design

For the matrix isolation studies, we used an APD Cryogenics HC-2 cryostat with a closed-cycle refrigerator system, equipped with an inner CsI window for IR measurements. Spectra were recorded using a Bruker IFS 55 FT-IR spectrometer with a spectral range of 4500–400 cm^{-1} and a resolution of 0.7 cm^{-1}, and UV/Vis spectra were recorded with a JASCO V-670 spectrophotometer. For the combination of high-vacuum flash pyrolysis with matrix isolation, we employed a small, home-built water-cooled oven, which was directly connected to the vacuum shroud of the cryostat. The pyrolysis zone consisted of an empty quartz

 This journal is © the Owner Societies 2022

Published on 30 May 2022. Downloaded by UNIVERSITAT GIESSEN on 8/21/2022 9:54:56 AM.

tube with an inner diameter of 8 mm, which was resistively heated over a length of 50 mm by a coaxial wire. The temperature was monitored with a NiCr–Ni thermocouple. At a distance of approximately 50 mm, all pyrolysis products were co-condensed with a large excess of argon (typically 60–120 mbar from a 2000 mL storage bulb) on the surface of the matrix window at 10 K. Several experiments with pyrolysis temperatures ranging from 650 °C were performed to determine the optimal pyrolysis conditions. A high-pressure mercury lamp (HBO 200, Osram) with a monochromator (Bausch & Lomb) was used for irradiation.

Computations

All geometries were optimized and characterized as minima utilizing analytic harmonic vibrational frequency computations at the UB3LYP/def2-QZVPP[45,46] level of theory. The grid size was defined with 99 radial shells and 590 angular points, and convergence criteria were set with the keyword "tight". All computations were performed with the Gaussian16 program package.[47] The NRT analysis was done using the NBO 7.0. program package.[43]

Conflicts of interest

No competing financial interests are declared.

Acknowledgements

Financial support by the Deutsche Forschungsgemeinschaft *via* grant MA 8773/3-1 is gratefully acknowledged. A. M. thanks Prof. Dr. Peter R. Schreiner for his continuous and generous support.

References

1 C. Chatgilialoglu and A. Studer, *Encyclopedia of Radicals in Chemistry, Biology and Materials*, John Wiley & Sons, Ltd., 2012.
2 J. Stubbe and D. G. Nocera, *J. Am. Chem. Soc.*, 2021, **143**, 13463–13472.
3 A. Mardyukov and P. R. Schreiner, *Acc. Chem. Res.*, 2018, **51**, 475–483.
4 H. M. McConnell and D. B. Chesnut, *J. Chem. Phys.*, 1958, **28**, 107–117.
5 R. W. Fessenden and R. H. Schuler, *J. Chem. Phys.*, 1963, **39**, 2147–2195.
6 T. Takada and M. Dupuis, *J. Am. Chem. Soc.*, 1983, **105**, 1713–1716.
7 H.-G. Korth, H. Trill and R. Sustmann, *J. Am. Chem. Soc.*, 1981, **103**, 4483–4489.
8 G. B. Ellison, G. E. Davico, V. M. Bierbaum and C. H. DePuy, *Int. J. Mass Spectrom. Ion Processes*, 1996, **156**, 109–131.
9 K. Kleinermanns and A. Luntz, *J. Phys. Chem.*, 1981, **85**, 1966–1968.
10 R. J. Buss, R. J. Baseman, G. He and Y. Lee, *J. Photochem.*, 1981, **17**, 389–396.
11 V. Schmidt, G.-Y. Zhu, K. Becker and E. Fink, *Ber. Bunsenges. Phys. Chem.*, 1985, **89**, 321–322.
12 H. Hunziker, H. Kneppe and H. Wendt, *J. Photochem.*, 1981, **17**, 377–387.
13 M. Dupuis, J. J. Wendoloski and W. A. Lester Jr., *J. Chem. Phys.*, 1982, **76**, 488–492.
14 L. F. DiMauro, M. Heaven and T. A. Miller, *J. Chem. Phys.*, 1984, **81**, 2339–2346.
15 M. Heaven, L. Dimauro and T. A. Miller, *Chem. Phys. Lett.*, 1983, **95**, 347–351.
16 M. E. Jacox, *Chem. Phys.*, 1982, **69**, 407–422.
17 J. D. Weidman, R. T. Allen, K. B. MooreI II and H. F. Schaefer III, *J. Chem. Phys.*, 2018, **148**, 184308.
18 K. O. MacFadden and C. L. Currie, *J. Chem. Phys.*, 1973, **58**, 1213–1219.
19 G. Inoue and H. Akimoto, *J. Chem. Phys.*, 1981, **74**, 425–433.
20 L. Zhu and G. Johnston, *J. Phys. Chem.*, 1995, **99**, 15114–15119.
21 M. Nakajima, T. W. Schmidt, Y. Sumiyoshi and Y. Endo, *J. Chem. Phys.*, 2009, **131**, 104310.
22 M. Yamaguchi, T. Momose and T. Shida, *J. Chem. Phys.*, 1990, **93**, 4223–4229.
23 P. Felder, E. A. J. Wannenmacher, I. Wiedmer and J. R. Huber, *J. Phys. Chem.*, 1992, **96**, 4470–4477.
24 M. Nakajima, A. Miyoshi, Y. Sumiyoshi and Y. Endo, *J. Chem. Phys.*, 2007, **126**, 044307.
25 Z. Wu, L. Wang, B. Lu, A. K. Eckhardt, P. R. Schreiner and X. Zeng, *Phys. Chem. Chem. Phys.*, 2021, **23**, 16307–16315.
26 S. Nehzati, N. V. Dolgova, D. Sokaras, T. Kroll, J. J. H. Cotelesage, I. J. Pickering and G. N. George, *Inorg. Chem.*, 2018, **57**, 10867–10872.
27 X. Wen, S. Wang, R. Liu, R. Duan, S. Hu, T. Jiao, L. Zhang and M. Liu, *Small*, 2022, **18**, 2104301.
28 L. Song, F. Keul and A. Mardyukov, *Chem. Commun.*, 2019, **55**, 9943–9946.
29 S. Yamago, K. Iida and J.-I. Yoshida, *J. Am. Chem. Soc.*, 2002, **124**, 2874–2875.
30 L. B. Han, K. Ishihara, N. Kambe, A. Ogawa, I. Ryu and N. Sonoda, *J. Am. Chem. Soc.*, 1992, **114**, 7591–7592.
31 H. Radford, *J. Chem. Phys.*, 1964, **40**, 2732–2733.
32 E. Fink, K. Setzer, D. Ramsay and M. Vervloet, *J. Mol. Spectrosc.*, 1989, **138**, 19–28.
33 D. A. Gillett, J. P. Towle, M. Islam and J. M. Brown, *J. Mol. Spectrosc.*, 1994, **163**, 459–482.
34 R. Donovan, D. Little and J. Konstantatos, *J. Chem. Soc., Faraday Trans. 2*, 1972, **68**, 1812–1818.
35 F. Keul, A. Mardyukov and P. R. Schreiner, *Phys. Chem. Chem. Phys.*, 2019, **21**, 25797–25801.
36 S. Yamago, K. Iida and J.-i Yoshida, *J. Am. Chem. Soc.*, 2002, **124**, 13666–13667.
37 S. Yamago, K. Iida, M. Nakajima and J.-I. Yoshida, *Macromolecules*, 2003, **36**, 3793–3796.
38 M. Dabdoub and J. Comasseto, *J. Organomet. Chem.*, 1988, **344**, 167–173.
39 A. Mardyukov and P. R. Schreiner, *Phys. Chem. Chem. Phys.*, 2016, **18**, 26161–26165.

Published on 30 May 2022. Downloaded by UNIVERSITAT GIESSEN on 8/21/2022 9:54:56 AM.

40 A. Mardyukov, Y. A. Tsegaw, W. Sander and P. R. Schreiner, *Phys. Chem. Chem. Phys.*, 2017, **19**, 27384–27388.
41 E. S. Kline, Z. H. Kafafi, R. H. Hauge and J. L. Margrave, *J. Am. Chem. Soc.*, 1985, **107**, 7559–7562.
42 M. Klussmann, *Chem. – Eur. J.*, 2018, **24**, 4480–4496.
43 E. D. Glendening, J. K. Badenhoop, A. E. Reed, J. E. Carpenter, J. A. Bohmann, C. M. Morales, P. Karafiloglou, C. R. Landis and F. Weinhold, 2018.
44 E. D. Glendening, C. R. Landis and F. Weinhold, *J. Comput. Chem.*, 2019, **40**, 2234–2241.
45 F. Weigend, *Phys. Chem. Chem. Phys.*, 2006, **8**, 1057–1065.
46 F. Weigend and R. Ahlrichs, *Phys. Chem. Chem. Phys.*, 2005, **7**, 3297–3305.
47 M. J. Frisch, G. W. Trucks, H. B. Schlegel, G. E. Scuseria, M. A. Robb, J. R. Cheeseman, G. Scalmani, V. Barone, G. A. Petersson, H. Nakatsuji, X. Li, M. Caricato, A. Marenich, J. Bloino, B. G. Janesko, R. Gomperts, B. Mennucci, H. P. Hratchian, J. V. Ortiz, A. F. Izmaylov, J. L. Sonnenberg, D. Williams-Young, F. Ding, F. Lipparini, F. Egidi, J. Goings, B. Peng, A. Petrone, T. Henderson, D. Ranasinghe, V. G. Zakrzewski, J. Gao, N. Rega, G. Zheng, W. Liang, M. Hada, M. Ehara, K. Toyota, R. Fukuda, J. Hasegawa, M. Ishida, T. Nakajima, Y. Honda, O. Kitao, H. Nakai, T. Vreven, K. Throssell, J. A. Montgomery, J. E. Peralta, F. Ogliaro, M. Bearpark, J. J. Heyd, E. Brothers, K. N. Kudin, V. N. Staroverov, T. Keith, R. Kobayashi, J. Normand, K. Raghavachari, A. Rendell, J. C. Burant, S. S. Iyengar, J. Tomasi, M. Cossi, J. M. Millam, M. Klene, C. Adamo, R. Cammi, J. W. Ochterski, R. L. Martin, K. Morokuma, O. Farkas, J. B. Foresman and D. J. Fox, *Gaussian 16 Rev. B.01*, Inc., Wallingford CT, 2016.

This journal is © the Owner Societies 2022

2.4 Further co-authored publications

1,1,2-Ethentriol: The enol of glycolic acid, a high-energy prebiotic molecule, A. Mardyukov, F. Keul, P. R. Schreiner, Angew. Chem. Int. Ed., **2021**, 60, 15313-15316. (DOI: 10.1002/ange.202104436)

Preparation and characterization of the enol of acetamide: 1-aminoethenol, a high-energy prebiotic molecule, A. Mardyukov, F. Keul, P. R. Schreiner, Chem. Sci., **2020**, 11, 12358-12363. (DOI: 10.1039/D0SC04906A)

Isolation and characterization of the free phenylphosphinidene chalgonides $C_6H_5P{=}O$ and $C_6H_5P{=}S$, the phosphorus analogues of nitrosobenzene and thionitrosobenzene, A. Mardyukov, F. Keul, P. R. Schreiner, Angew. Chem. Int. Ed., **2020**, 59, 12445-12449. (DOI: 10.1002/anie.202004172)

Preparation and spectroscopic identification of methyl-Se-nitroselenol, L. Song, F. Keul, A. Mardyukov, Chem. Commun., **2019**, 55, 9943-9946. (DOI: 10.1039/C9CC05065E)

Generation and spectroscopic identification of the thiuram radical $(CH_3)_2NCS_2$, A. Mardyukov, F. Keul, P. R. Schreiner, J. Phys. Chem. A, **2019**, 123, 4937-4941. (DOI: 10.1021/acs.jpca.9b03307)

Preparation and characterization of phenyl phosphine diselenide – the monomeric form of Woollin´s reagent, A. Mardyukov, F. Keul, P. R. Schreiner, Eur. J. Org. Chem., **2019**, 2-3, 387-390. (DOI: 10.1002/ejoc.201800639)

3 Acknowledgment – Danksagung

Während meines Studiums und meiner Promotionszeit durfte ich zahlreiche Personen kennenlernen, ohne deren Unterstützung diese Doktorarbeit so nicht möglich gewesen wäre:

Prof. Dr. Peter R. Schreiner, PhD für die Aufnahme in seinen Arbeitskreis und die Übernahme der Betreuung für meine Promotion sowie für die stete Unterstützung in allen Projekten, nicht nur während der Promotion, sondern auch schon im Studium. Weiterhin danke ich für das entgegengebrachte Vertrauen und die gegebenen Freiheiten in meiner Forschung.

Prof. Dr. Bernd Smarsly für die Übernahme und Anfertigung eines Zweitgutachtens für diese Arbeit.

Dr. Artur Mardyukov für die Zusammenarbeit in zahllosen Projekten, für die Unterstützung in meinen Projekten und vielen fruchtvollen Diskussionen. Neben dessen gilt ihm auch mein Dank für spannende Schachpartien.

Dr. Christian Eschmann für die gute Betreuung während meiner Vertiefung und Spezialisierung, aber auch vor allem während meiner Master-Thesis.

Dr. Raffael C. Wende und **Dr. André K. Eckhardt** für die Zusammenarbeit an verschiedenen *origin of life* Projekten, für eine gute Zusammenarbeit in B207, anregende Diskussionen und eine gute Laboratmosphäre.

Dr. Dennis Gerbig und **Dr. Henrik Quanz** für die Geduld bei der Beantwortung meiner vielen Fragen bezüglich Computational Chemistry.

Ein weiterer Dank geht an meine (ehemaligen) Labor- und Bürokollegen **Dr. André K. Eckhardt**, **Lijuan Song, PhD**, **Ephrat Solel, PhD**, **Dr. Henrik Quanz**, **Weiyu Qian**, **Guanqi Qiu, PhD** und **Dr. Raffael C. Wende** für die unterhaltsame Zeit und die tolle Arbeitsatmosphäre.

Alexander Seitz für die hervorragende Vorbereitung auf das Studium während der Einführungswoche im Wintersemester 12/13.

Simon Hofmann für die stets ordentlich durchgeführten Synthesen von organischen Verbindungen.

Meinen (ehemaligen) Arbeitskollegen **Dr. Christian Eschmann**, **Jan M. Schümann**, **Dr. Frederik R. Erb**, **Markus Schauermann**, **Alexander Seitz**, **Henrik F. König**, **Dr. Bastian Bernhardt** und **Lars Rummel** danke ich für unterhaltsame Kaffeepausen und abendliche Treffen.

Der **gesamten PRS-Group** für die nette Arbeitsatmosphäre.

Edgar Reitz für den unermüdlichen Kampf gegen technische Probleme.

Anja Beneckenstein für die schnelle Reparatur des ein oder anderen kaputten Glasgerätes und das Lösen von hartnäckig festgeklemmten Schliffen.

Dr. Jörg Neudert, **Frau Richter** und **Frau Jäger** für sämtliche administrativen Aufgaben.

Ein weiterer Dank gilt dem **Institut für Organische Chemie** für die Bereitstellung der Räumlichkeiten und Arbeitsmaterialien.

Mein Dank gilt auch **der gesamten OC-Analytik** für das schnelle Messen unzähliger Proben.

Dr. Bastian Bernhardt, **Marcel Ruth**, **Alexander Granichny** für anstrengende Abende im Level8.

Meinen Studienkollegen **Tobias Hollubarsch**, **Dr. Thorben Krauskopf**, und **Tim Weber** für die schöne, unterhaltsame Zeit während des Studiums und dass wir die Praktika lebend beendet haben.

Meinen **Eltern** für ihre gesamte Unterstützung nicht nur während des Studiums, sondern auch schon in meinen Kindheitstagen für die Förderung von all meinen Interessen.

Meiner Frau **Hannah** für die Unterstützung in allen Lebenslagen und das Aushalten aller Widrigkeiten, die das Anfertigen einer Promotionsarbeit mit sich bringt.